Imperial College London

Imperial College London

Department of Mathematics

The Importance of Discrete Dynamic Risk Constraints for Controlling Tail-risk Seeking Traders

Author: Baofeng Ye (CID: 01918592)

A thesis submitted for the degree of

MSc in Mathematics and Finance, 2019-2020

Declaration

The work contained in this thesis is my own work unless otherwise stated.

Acknowledgements

First of all, I would like to thank my supervisor, professor Damiano Brigo who introduced me to the facts of utility optimisation under risk constraints, and provided invaluable guidance and comments along the way. And I sincerely hope that he will get better soon.

I would also like to thank the whole MSc Mathematics and Finance team for the exciting and engaging courses and materials they offer.

I am very grateful to my parents for their unconditional support thought this academic year.

My last thank goes to my fiancee Yueshan for the wonderful time we shared during our whole journey in Imperial College.

Abstract

Previous studies have shown that static risk constraints based on prevalent risk measures, such as Value at Risk and Expected Shortfall, are ineffective to curb the maximal expected utility of a tail-risk-seeking trader with an S-shaped utility function under portfolio optimisation problems while imposing constraints throughout the whole trading period can reduce the achieved utility effectively. This paper shows that the maximal expected utility can be bounded to an acceptable level when a finite number of checking times are imposed. We do so by extending the original Least-Square Monte Carlo method to endogenous states and transforming the utility to reduce the simulation bias. The simulation study results of different economy models and utility functions conclude our findings, and the extended method can be applied to general utility optimisation problems with S-shaped utility if a differentiable and invertible transformation function exists.

Contents

List of Figures

List of Tables

Introduction

Portfolio optimisation has generally been expressed as the problem of maximising expected utility function under the expected utility hypothesis. This hypothesis states that the expected value of the utility function will be the most representative of the utility at any given point in time in the face of uncertainty. The main issue with this optimisation problem is that a uniquely correct way of quantifying utility may not exist. A general way is to assume that the individual is risk-averse, which implies that the utility function should be concave and diminishing marginal wealth utility. However, the concave assumption may not be adequate to model the behaviour of an agent's preferences in a real trading environment. Kahneman & Tversky (2013) state that individuals may be risk-seeking over positive loss while keeps the risk-averse behaviour over positive payoff. Follow with Armstrong et al. (2020), this paper also considers the traders with 'tail-risk-seeking' behaviour who are less concerned with extremal losses and hence their utility function is assumed to be S-shaped.

Armstrong & Brigo (2019*b*) show a surprising result that the Value at Risk (VaR) and Expected Shortfall (ES) is completely ineffective to limit the risk-seeking behaviour of the tail-risk-seeking trader. They proved this result through a portfolio optimisation problem with S-shaped utility under static risk constraints. It turned out that neither VaR nor ES can change the maximum expected utility achieved by a trader who is seeking tail risk, compared to the case without any risk constraint. An earlier version of this conclusion is driven by Armstrong & Brigo (2018), which only considers the Black-Scholes market. Armstrong & Brigo (2019*a*) show that the positive homogeneity of the risk measure is the main reason that causes this problem. They introduce a kind of portfolio that is with non-positive price and non-positive risk but with positive probability to being strictly positive measured by a coherent risk measure ρ and call this as ρ-arbitrage and call the risk measure as ineffective if a static risk constraint from this risk measure cannot reduce the expected utility of a trader with limited liability. The ineffectiveness of a static risk constraint is proved to be equivalent to the existence of the corresponding ρ-arbitrage under the given coherent risk measure ρ. Armstrong et al. (2020) show that if the risk constraint is instead dynamic, that is, the risk constraint is imposed throughout the entire trading horizon, the maximal expected utility achieved can be reduced. They estimate the portfolio risk at each evaluation time by introducing an evaluation window under the assumption that the assets holding is unchanged. The emphasis for us, is that though the dynamic risk constraint can bound the maximal expected utility effectively if the constraint is imposed through the whole trading horizon, the efficiency of a single risk constraint during the horizon remains unknown. Furthermore, whether the dynamic risk constraint can still reduce the maximal expected utility if the constraint is imposed only in some of the evaluation time but not the whole trading period is also unknown.

We thus explore a simple modification to the stochastic optimisation problem introduced by Armstrong et al. (2020). The risk measure is still imposed dynamically but only on a finite number of checking points throughout the trading horizon. It turns out that the modified optimisation problem can be re-written as a stochastic control problem with an endogenous state and a dynamic risk constraint that differs through the trading period. Analytical solutions are limited to this type of control problem with few stochastic factors and limitations on the dynamics. Simulation approach, therefore, has become a field of active research activity due to its flexibility over the number of variables and stochastic factors. One of the simulation methods that has been developed extensively recently is the Least-Squares Monte Carlo (LSMC) method due to its flexibility in the dynamics of underlying processes and restrictions on constraints. This algorithm generally contains a forward simulation process, and a backward optimisation process where regression is performed to approximate the value function. When applying the method to endogenous state variables, the simulation becomes complicated as the future state will be affected by current con-

trol. Another problem is that the basis function for regression in the backward optimisation is difficult to find when the objective function is based on utility functions. Non-appropriate basis functions will rapidly amplify the error of the regression and blow up the solution. Andreasson & Shevchenko (2019) provides a possible approach to the standard discrete dynamic programming problem with concave utility function. We extend this method to the S-shaped utility optimisation problem we face. Following Andreasson & Shevchenko (2019), we propose to transform the utility function to improve the fit, then try to avoid the re-transform bias caused by the non-linearity of the transformation function. In order to improve the exploration of the state space, instead of simulating continuous process path, we conduct a re-sampling on the state variable when performing the forward simulation process.

Our main contribution is to show that the maximal expected utility is indeed decreasing as the number of checking points increases with the VaR or ES constraint, in the sense that although the efficiency of the risk constraint is highly depend on the shape of the utility function, adding enough checking points can still bound the maximal expected utility to an acceptable level. Besides, the extended LSMC algorithm we introduce can deal with general portfolio optimisation problems with flexible risk constraints although the computational amount is large.

We conclude the introduction by the organisation of this paper. A glossary is given after this introduction to better explain the symbols we use in the paper. Chapter 1 gives the two economy cases we consider. Chapter 2 introduces the extended LSMC method for our stochastic control problem. The detailed discussion with simulated results of the two economy cases is in Chapter 3. Then, a conclusion is given as an end of this paper. Supporting materials are deferred to the appendix.

Glossary

τ : a positive number that represents the current checking time.

Θ_Z : $\{\tau_i \in (0,T) : i = 1, \ldots, Z, Z \in \mathbb{Z}\}$, the set of checking times.

ρ : a function that obeys the definition of risk.

$\cdot^E$: $E \in \{J, B\}$, the superscript means that $\cdot$ is under the corresponding economy case, J represents the case with jump process and B represents the one with a geometric Brownian Motion.

Π : an admissible process that represents a portfolio strategy.

X : a stochastic process that represents the value of a portfolio.

$\boldsymbol{\Delta}$: a small positive number that represents an evaluation window by the portfolio manager.

L : a stochastic process that represents the estimated loss of a portfolio given the evaluation window $\boldsymbol{\Delta}$.

$X(\Pi)$: the symbol (Π) states that the portfolio is affected by the control Π. This symbol is dropped after section 2.1 for symbol simplification.

$\Delta\cdot$: the change of movement of $\cdot$ in a small time scale.

K : a set of portfolio strategies under a given constraint.

$\mathcal{A}(K)$: a set of admissible portfolio strategies with a given dynamic risk constraint.

$\Phi(\cdot)$: a real-value function that represents the approximated conditional expectation of the value function from a stochastic control problem.

$T(\cdot)$: an invertible real-value function that represents the transformation we apply to the utility.

$\mathcal{T}_t(\cdots)$: a real-value function that represents the evolution of a portfolio from time t to the time $t + \boldsymbol{\Delta}$.

Chapter 1

Model setup

For simplicity of exposition, we consider two economy cases, each of which is with one risk-free bond and one risky asset. The risk-free rate is assumed to be r. Let $(\Omega, \mathcal{F}, \{\mathcal{F}_t\}_{0\le t\le T}, \mathbb{P})$ be a filtered probability space with a fixed terminal horizon $T > 0$ that supports a one-dimensional Brownian Motion $W = (W_t)_{t\ge 0}$. The two risky assets are defined to be a jump process of 'discrete' geometric Brownian Motion type and a standard geometric Brownian Motion, respectively. A dynamic risk constraint is imposed such that $\rho(L_\tau) \le R$ with confidence level α for some checking times $\tau \in \{\tau_i \in (0,T) : i = 1, \dots, Z, Z \in \mathbb{Z}\} =: \Theta_Z$, where L_τ is the loss at time τ, $\rho(\cdot)$ denotes some risk measure and R is an exogenous limit of risk.

1.1 The economy with a jump process

The price process $S^J = \left(S^J{}_t\right)_{t\ge 0}$ of the risky asset, in this case, is defined to follow a 'discrete' geometric Brownian Motion in the form of

$$\begin{aligned}
S^J{}_0 &= s^J{}_0,\\
\log S^J{}_{T/2} &= \log S^J{}_0 + \left(\mu^J - \frac{\sigma^J{}^2}{2}\right)\frac{T}{2} + \sigma^J\sqrt{T/2}\varepsilon_1,\\
\log S^J{}_T &= \log S^J{}_{T/2} + \left(\mu^J - \frac{\sigma^J{}^2}{2}\right)\frac{T}{2} + \sigma^J\sqrt{T/2}\varepsilon_2,
\end{aligned}$$

with initial price $s^J{}_0$, drift μ^J and volatility $\sigma^J > 0$, where ε_1 and ε_2 are two independent variables following the standard Normal distribution.

A trader is assumed to invest in the risky and risk-free assets dynamically with an amount of $\Pi^J{}_t$ into the risky one at time t. The portfolio strategy $\Pi^J = \left(\Pi^J{}_t\right)_{t\ge 0}$ is set to be admissible, i.e. it's adapted and $\int_0^T \Pi^J{}_t^2 dt < \infty$ almost surely. The set of admissible portfolio strategies is then denoted as $\mathcal{A}^J{}_0$. The value of the portfolio $X^J{}_t$ at time t can then be expressed as

$$dX^J{}_t = \frac{\Pi^J{}_t}{S^J{}_t}\Delta S^J{}_t + r\left(X^J{}_t - \Pi^J{}_t\right)dt, \quad X^J{}_0 = x^J{}_0, \tag{1.1.1}$$

where $x^J{}_0$ is an exogenously initial capital from the trader and $\Delta S^J{}_t$ is defined as

$$\begin{aligned}
\Delta S^J{}_t &:= S^J{}_t - S^J{}_{t^-}\\
&= \exp(\log S^J{}_t) - \exp(\log S^J{}_{t^-})\\
&= \exp(\log S^J{}_t)[1 - \exp(-\Delta \log S^J{}_t)],
\end{aligned}$$

where $\Delta \log S^J{}_t = \log S^J{}_t - \log S^J{}_{t^-}$. Then by the Itô's integral of jump process, we have

$$X^J{}_{t+\mathbf{\Delta}} = e^{r\mathbf{\Delta}}X^J_c{}_t - e^{r\mathbf{\Delta}}\Pi^J{}_t + \Pi^J{}_t\exp(\Delta \log S^J{}_t)$$

for any t and $\mathbf{\Delta} > 0$, where $X^J_c{}_t$ is defined by $dX^J_c{}_t = r\left(X^J_c{}_t - \Pi^J{}_t\right)dt$. Then the difference between $X^J{}_{t+\mathbf{\Delta}}$ and $e^{r\Delta}X^J{}_t$,

$$X^J{}_{t+\mathbf{\Delta}} - e^{r\Delta}X^J{}_t = -e^{r\mathbf{\Delta}}\Pi^J{}_t + \Pi^J{}_t\exp(\Delta \log S^J{}_t) \tag{1.1.2}$$

can be interpreted as the portfolio loss in the time horizon $[t, t+\boldsymbol{\Delta}]$.

At each time t, the portfolio manager assesses the risk which given from equation (1.1.2). Suggested by Yiu (2004), we suppose that under normal circumstances, the manager only has the information of the investor's strategy Π^J up to current time t, and he assumes Π^J to be fixed during the evaluation window $[t, t+\boldsymbol{\Delta}]$. Then the loss of the portfolio over $[t, t+\boldsymbol{\Delta}]$ estimated at time t, denoted as ${L^J}_t$, is given by

$$ {L^J}_t = e^{r\boldsymbol{\Delta}} {\Pi^J}_t - {\Pi^J}_t \exp(\Delta \log {S^J}_t). $$

Notice that the price of the risky asset ${S^J}_t$ at time t only changes in time horizons $[\frac{T}{2}-\delta, \frac{T}{2}+\delta]$ and $[T-\delta, T]$ for any small $\delta \in \mathbb{R}^+$, in other time it's simply $e^{r\boldsymbol{\Delta}}{\Pi^J}_t$. In $[\frac{T}{2}-\delta, \frac{T}{2}+\delta]$ and $[T-\delta, T]$, we have

$$ \Delta \log {S^J}_t = \left(\mu^J - \frac{{\sigma^J}^2}{2}\right)\frac{T}{2} + \sigma^J \sqrt{T/2}\varepsilon, \tag{1.1.3} $$

where $\varepsilon \sim N(0,1)$. Hence, the estimated loss in these two horizons follow

$$ \left[\log(-\frac{1}{{\Pi^J}_t}{L^J}_t + e^{r\boldsymbol{\Delta}}) - \left(\mu^J - \frac{{\sigma^J}^2}{2}\right)\frac{T}{2}\right]\frac{1}{\sigma^J\sqrt{T/2}} \sim N(0,1). $$

Remark 1.1.1. There are different ways to estimate the loss of the portfolio. We can alternatively assume that the proportion of the amount invested in the risky asset, ${\Pi^J}_t/{X^J}_t$, to be fixed, recommended by Cuoco et al. (2008). In this approach, the distribution of ${L^J}_t$ also depends on the current value ${X^J}_t$, which causes a more complicated and computational heavy problem. Thus we only focus on the approach by Yiu (2004).

From equation (1.1.3), $\Delta \log {S^J}_t$ is normally distributed, leading to a shifted log-normal distribution of the loss ${L^J}_t$ for time t in $[\frac{T}{2}-\delta, \frac{T}{2}+\delta]$ and $[T-\delta, T]$ and hence the evaluating point t that is neighbour to time $T/2$ and T if the evaluation window contains the time $T/2$ and T. Though shifted log-normal distribution is not as convenient a property as normal distribution, we can still solve for the quantile with desired confidence levels numerically, and hence the corresponding Value-at Risk (VaR) which is defined as $\mathrm{VaR}_\alpha(L_t) := \sup\{x \in \mathbb{R} : \mathbb{P}(L_t \geq x) > \alpha\}$. In other time horizon, $\mathrm{VaR}_\alpha\left({L^J}_\tau(\pi)\right)$ is simply equal to the loss, since ${L^J}_\tau(\pi)$ is constant at given time $\tau \notin [\frac{T}{2}-\delta, \frac{T}{2}+\delta] \cup [T-\delta, T]$ with $\delta > 0$, and the maximal value that is not greater than ${L^J}_\tau(\pi)$ is the loss itself. We then define the constraint set

$$ K^J_{\mathrm{VaR}} := \left\{\pi \in \mathbb{R} : \mathrm{VaR}_\alpha\left({L^J}_\tau(\pi)\right) \leq R, \tau \in \Theta_Z\right\} $$

such that the constraint deduced from VaR at time τ is equivalent to ${\Pi^J}_\tau \in K^J_{\mathrm{VaR}}$. Expected Shortfall (ES) is defined to be $\mathrm{ES}_\alpha(L_t) := \mathbb{E}[L_t \mid L_t \geq \mathrm{VaR}_\alpha(L_t)]$ which can only be numerically evaluated with loss ${L^J}_t$. Due to the huge computational amount when performing the algorithm in Chapter 2, we do not take it into consideration in this economy case.

1.2 The economy with a geometric Brownian Motion

We now consider the price process $S^B = \left({S^B}_t\right)_{t\geq 0}$ of the risky asset to have a geometric Brownian Motion

$$ d{S^B}_t = \mu {S^B}_t dt + \sigma {S^B}_t dB_t $$

with initial value ${S^B}_0 = 0$, drift μ^B and volatility $\sigma^S > 0$. The portfolio strategy $\Pi^B = \left({\Pi^B}_t\right)_{t\geq 0}$ is still assumed to be admissible, and fix at every evaluation window $[t, t+\boldsymbol{\Delta}]$. Then the set of admissible portfolio strategies in this case is denoted as ${\mathcal{A}^B}_0$. Hence the portfolio value process $X^B = \left({X^B}_t\right)_{t\geq 0}$ is evolved as

$$ \begin{aligned} d{X^B}_t &= \frac{{\Pi^B}_t}{{S^B}_t} d{S^B}_t + r\left({X^B}_t - {\Pi^B}_t\right)dt \\ &= \left[r{X^B}_t + {\Pi^B}_t(\mu^B - r)\right]dt + {\Pi^B}_t \sigma^B dW_t \end{aligned} \tag{1.2.1} $$

with exogenous initial capital ${X^B}_0 = {x^B}_0$, which is an Ornstein–Uhlenbeck process. Hence we can deduce

$${X^B}_{t+\boldsymbol{\Delta}} - e^{r\boldsymbol{\Delta}} {X^B}_t = (\mu^B - r) \int_t^{t+\boldsymbol{\Delta}} e^{r(t+\boldsymbol{\Delta}-s)} {\Pi^B}_s ds + \sigma^B \int_t^{t+\boldsymbol{\Delta}} e^{r(t+\boldsymbol{\Delta}-s)} {\Pi^B}_s dW_s$$

for any t and $\boldsymbol{\Delta} > 0$. Based on Yiu (2004), the loss ${L^B}_t$ of the portfolio is of the form

$$\begin{aligned} {L^B}_t &= (r - \mu^B) \int_t^{t+\boldsymbol{\Delta}} e^{r(t+\boldsymbol{\Delta}-s)} {\Pi^B}_s ds - \sigma^B \int_t^{t+\boldsymbol{\Delta}} e^{r(t+\boldsymbol{\Delta}-s)} {\Pi^B}_s dW_s \\ &= \frac{(r-\mu^B)\left(e^{r\boldsymbol{\Delta}} - 1\right)}{r} \Pi_t^B - \sigma^B \Pi_t^B \int_t^{t+\boldsymbol{\Delta}} e^{r(t+\boldsymbol{\Delta}-s)} dW_s \end{aligned}$$

which follows a normal normal distribution with the mean and the variance

$$\mathbb{E}\left[{L^B}_t\right] = -\frac{(\mu^B - r)\left(e^{r\boldsymbol{\Delta}} - 1\right)}{r} {\Pi^B}_t, \quad \mathrm{Var}\left({L^B}_t\right) = \frac{\left(e^{2r\boldsymbol{\Delta}} - 1\right){\sigma^B}^2}{2r} {\Pi^B}^2_t.$$

By the similar approach as in section 1.1, we can define the constraint set for Π^B by setting the risk measure to be VaR and ES, denoted K^B_{VaR} and K^B_{ES},

$$K^B_{\mathrm{VaR}} := \left\{ \pi \in \mathbb{R} : -\frac{(\mu^B - r)\left(e^{r\boldsymbol{\Delta}} - 1\right)}{r} \pi - \sigma^B \sqrt{\frac{e^{2r\boldsymbol{\Delta}} - 1}{2r}} \Phi^{-1}(\alpha) |\pi| \leq R \right\} \tag{1.2.2}$$

$$K^B_{\mathrm{ES}} := \left\{ \pi \in \mathbb{R} : -\frac{(\mu^B - r)\left(e^{r\boldsymbol{\Delta}} - 1\right)}{r} \pi + \sigma^B \sqrt{\frac{e^{2r\boldsymbol{\Delta}} - 1}{2r}} \frac{\phi\left(\Phi^{-1}(\alpha)\right)}{\alpha} |\pi| \leq R \right\}, \tag{1.2.3}$$

$$\tag{1.2.4}$$

where $\Phi(\cdot)$ is the cumulative distribution function of the standard normal distribution, and $\phi(\cdot)$ is the corresponding probability density function. The risk constraints deduced from VaR and ES at time τ are again equivalent to ${\Pi^B}_\tau \in K^B_{\mathrm{VaR}}$ and ${\Pi^B}_\tau \in K^B_{\mathrm{ES}}$ respectively. We now state the lemma from Armstrong et al. (2020), which shows that in this economy case, the efficiency of these two constraints are related to the proportion of $(\mu^B - r)$ over σ^B, and the value of the confidence level α and time step $\boldsymbol{\Delta}$.

Lemma 1.2.1. *(Armstrong et al. (2020), Lemma 1) Define the constants*

$$M_{VaR} := -\sqrt{\frac{e^{2r\boldsymbol{\Delta}} - 1}{2r}} \frac{r}{e^{r\boldsymbol{\Delta}} - 1} \Phi^{-1}(\alpha) > 0, \quad M_{ES} := \sqrt{\frac{e^{2r\boldsymbol{\Delta}} - 1}{2r}} \frac{r}{e^{r\boldsymbol{\Delta}} - 1} \frac{\phi\left(\Phi^{-1}(\alpha)\right)}{\alpha} > 0.$$

Then for $i \in \{VaR, ES\}$, the sets K_i^B defined in (1.2.4) *have the following properties,*

- *if $\frac{\mu^B - r}{\sigma^B} \geq M_i$, then there exists $-\infty < k_1^i < 0$ such that $K_i^B \in [k_1^i, \infty)$,*
- *if $\left|\frac{\mu^B - r}{\sigma^B}\right| < M_i$, then there exists $-\infty < k_1^i < 0 < k_2^i < \infty$ such that $K_i^B = \left[k_1^i, k_2^i\right]$,*
- *if $\frac{\mu^B - r}{\sigma^B} \leq M_i$, then there exists $0 < k_2^i < \infty$ such that $K_i^B = \left(-\infty, k_2^i\right]$.*

1.3 S-shaped utility function and optimisation problem

We assume that the trader is of 'tail-risk-seeking' type who is not sensitive to extremal losses with S-shaped utility function $U(\cdot)$. The trader is supposed to maximise his expected utility of the terminal portfolio value. We also adopt the assumption given by Armstrong et al. (2020),

Assumption 1.3.1. (Armstrong et al. (2020), Assumption 1) The utility function U is continuous, increasing and concave (resp. convex) on $x > 0$ (resp. $x < 0$) with $U(0) = 0$ and $\lim_{x \to -\infty} \frac{U(x)}{x} = 0$.

Note that the utility function $U(\cdot)$ can be non-differentiable. Under the assumption, the trader is risk averse in the domain of positive profit and risk seeking over the domain of loss. Moreover, the 'tail-risk-seeking' behaviour of the trader can be shown from the sub-linear growth of the utility function during extremal losses.

The underlying optimisation problem can then be expressed as

$$V(t,x) := \sup_{\Pi \in \mathcal{A}(K)} \mathbb{E}^{(t,x)} \left[U\left(X_T(\Pi) \right) \right] \tag{1.3.1}$$

where $X_T(\Pi)$ is of the dynamic given by (1.1.1) or (1.2.1), and $\mathcal{A}(K)$ is defined to be the corresponding admissible set of portfolio strategies with a given dynamic risk constraint,

$$\mathcal{A}(K) := \{\Pi \in \mathcal{A}_0 : \Pi(t,\omega) \in K \quad \mathcal{L} \otimes \mathbb{P} - \text{ a.e. } (t,\omega)\}$$

where K is some given set and $\mathcal{L}$ is the Lebesgue measure. If the risk constraint is absent, then we set $K = K_0 := \mathbb{R}$, and if the dynamic risk constraint is in place, we set $K \in \{K^J_{\text{VaR}}, K^B_{\text{VaR}}, K^B_{\text{ES}}\}$.

Let $V_K(t,x)$ be the value function of problem (1.3.1) where $K \in \{K_0, K^J_{\text{VaR}}, K^B_{\text{VaR}}, K^B_{\text{ES}}\}$ reflects the dynamic risk constraint and the economic model to be taken. The proposition from Armstrong et al. (2020), shown as proposition 1.3.2, indicates that by replicating a set of digital options with a large probability to gain and a small probability to have extremal losses, the tail-risk-seeking trader can achieve arbitrarily high utility if there is no constraint on the strategy.

Proposition 1.3.2. *(Armstrong et al. (2020), proposition 1) The value function of the unconstrained portfolio optimisation problem is* $V_{K_0}(t,x) = \sup_s U(s)$.

If a static constraint is taken to the terminal portfolio value,Armstrong & Brigo (2019*b*) proved that the trader can still attain an extremely high utility by manipulate the digital structure. Armstrong et al. (2020) show that if a dynamic constraint is adopted through the whole trading process, i.e. applying the constraint to the strategy Π_t at all time $t \in [0,T)$, the maximal expected utility can be constrained.

We are interested in investigating whether the maximum expected utility would still be bounded if the risk constraint were applied only at some discrete checking time $\tau \in \Theta_Z$ throughout the trading process.

Note that the portfolio optimisation problem of the form (1.3.1) with $U(\cdot)$ being S-shaped and constraints for all time $t \in [0,T)$ is studied by Armstrong et al. (2020) through analysing the performance of the corresponding HJB equations. Their results are not applicable to our settings as our constraint is not applied through the whole trading process. Basak & Shapiro (2001) studied the dynamic portfolio management problem based on the VaR constraint but the risk constraint imposed is static, which is not suitable for our model. Dong & Zheng (2019) also consider the problem with S-shaped utility, and with the strategy set K being a convex cone which is not the case in our model suggested by 1.2.1. Another problem is that due to the discrete behaviour of our checking process, the value function is analytically unsolvable in most of the cases due to the complexity of the dynamics of the risky asset, and hence the portfolio value under the effect of the risk constraint. Thus we seek to solve the corresponding optimisation problem numerically.

Chapter 2

Least-Squares Monte Carlo method with transformed utility

Notice that based on our setting in Chapter 1, the portfolio optimisation problem (1.3.1) is a multi-period stochastic control problem with state process $X_T(\Pi)$ and control Π. Due to the discrete type of the constraint in time, we turn to the Least-Squares Monte Carlo (LSMC) method as it imposes fewer restrictions on the constraint and underlying process. Since the original LSMC method, developed by Longstaff & Schwartz (2001), only provides simulation to exogenous states which differs from our model, we consider a more general case containing both exogenous and endogenous states, and perform a transform to the utility function, then try to avoid the re-transform bias.

2.1 Problem definition

With the fixed time horizon T, we divide the interval $[0, T]$ into n equal sub-intervals with grid points $0 = t_0 < t_1 < \ldots < t_n = T$ satisfying $t_i = i\boldsymbol{\Delta}, i = 0, \ldots n$ and $\boldsymbol{\Delta}$ is the evaluation window of the portfolio manager. Let $(\Omega, \mathcal{F}, \{\mathcal{F}_t\}_{0\leq t\leq T}, \mathbb{P})$ be, as in Chapter 1, the filtered probability space where $\mathcal{F}_t$ contains the necessary information up to time t. We only consider the processed which are well-defined and adapted to $\{\mathcal{F}_t\}_{0\leq t\leq T}$. The portfolio strategy $\Pi = (\Pi_{t_i})_{t_i, i=0,\ldots,n}$ can be regarded as the control which takes value in the admissible set $\mathcal{A}(K)$. We also let $Z = (Z_{t_i})_{t_i, i=1,\ldots,n} \in \mathcal{Z}$ be the perturbation term with realisation z_t. Then $X(\Pi) = (X_t(\Pi))_{t_i, i=0,\ldots,n} \in \mathcal{X}$ is the controlled state variable with evolution function

$$X_{t_{i+1}}(\Pi) = \mathcal{T}_{t_i}\left(X_{t_i}(\Pi), \Pi_{t_i}, Z_{t_{i+1}}\right),$$

interpreting that the state in the next period depends on the current state, the current control and the realisation of the perturbation term.

The multi-period dynamic optimisation problem (1.3.1) can be re-formulated as

$$V_0(X_0) = \sup_{\Pi\in\mathcal{A}(K)} \mathbb{E}\left[U\left(X_T(\Pi)\right) \mid X_0, \Pi\right].$$

In general, optimizing with respect to all controls $\Pi \in \mathcal{A}(K)$ at one run is difficult. A possible solution to simplify the calculation is through backward recursion by Bellman dynamic programming principle Bellman (1966) which transforms a multi-period optimisation problem into several single-period problems. If the value $U\left(X_T(\Pi)\right)$ is known at time T, then the optimal control $\Pi^*_{T-\boldsymbol{\Delta}}$ at time step $T - \boldsymbol{\Delta}$ can be generated by

$$\Pi^*_{T-\boldsymbol{\Delta}} = \arg\sup_{\Pi_{T-\boldsymbol{\Delta}}\in\mathcal{A}(K)} \mathbb{E}\left[U\left(X_T(\Pi)\right) \mid X_{T-\boldsymbol{\Delta}}, \Pi_{t-\boldsymbol{\Delta}}\right],$$

leading to the value function at time $T - \boldsymbol{\Delta}$,

$$V_{T-\boldsymbol{\Delta}}(x) = \mathbb{E}\left[U\left(X_T(\Pi)\right) \mid X_{T-\boldsymbol{\Delta}}(\Pi) = x, \Pi^*_{T-\boldsymbol{\Delta}}\right].$$

The multi-period stochastic control problem can then be solved with backward recursion, and the value functions at sequential time steps read

$$V_{t_i}(x) = \sup_{\Pi_t\in\mathcal{A}(K)} \mathbb{E}\left[V_{t_{i+1}}\left(X_{t_{i+1}}(\Pi)\right)\right) \mid X_{t_i}(\Pi) = x; \Pi_{t_i}\Big], i = n-1, \ldots, 0$$
$$V_{t_n}(x) = U(x).$$

This simplified problem is again normally not solvable analytically and still requires numerical methods. As the complexity of the underlying stochastic process increases, the computation amount of the numerical solution blows up rapidly. In the most straightforward cases, the state variable is not affected by the control, that is $X_t(\Pi) = X_t$, the LSMC method is then to approximate the conditional expectation $\Phi_{t_i}(X_{t_i})$ with the form

$$\Phi_{t_i}(X_{t_i}) = \mathbb{E}\left[V_{t_{i+1}}\left(X_{t_{i+1}}\right) \mid X_{t_i}\right]$$

by some basis function with independent variable X_{t_i} and response variable $V_{t_{i+1}}\left(X_{t_{i+1}}\right)$, denoted $\hat{\Phi}_{t_i}(X_{t_i})$. If the state is affected by the control, by Kharroubi et al. (2014), the conditional expectation

$$\Phi_{t_i}(X_{t_i}(\Pi), \Pi_{t_i}) = \mathbb{E}\left[V_{t_{i+1}}\left(X_{t_{i+1}}(\Pi)\right) \mid X_{t_i}(\Pi), \Pi_{t_i}\right]$$

could be estimated with regression over $X_{t_i}(\Pi)$ and randomised Π_{t_i}. For simplification, the symbol (Π) will be dropped from notations of the kind $X(\Pi)$ in the rest of the paper unless specified.

2.2 Basis functions and transformed utility

Besides ordinary polynomials, which is the simplest basis function, we also state several commonly used orthogonal basis in table 2.1, including Chebyshev, Laguerre, Legendre and Hermite polynomials.

Polynomial	$f_0(x)$	$f_1(x)$	$f_n(x)$
Chebyshev	1	x	$2xf_{n-1}(x) - f_{n-2}(x)$
Laguerre	1	$1-x$	$\frac{(2(n-1)+1-x)f_{n-1}(x)-(n-1)f_{n-2}(x)}{n}$
Legendre	1	x	$\frac{1}{2^n n!} dx^n \left(x^2-1\right) n$
Hermite	1	x	$(-1)^n e^{-x^2} \frac{d^n}{dx^n}\left(e^{-x^2}\right)$

Table 2.1: Basis functions that are commonly used in research.

Note that all these basis functions can only work globally only when the approximated function is strictly convex or concave. When the value function is based on some non-linear utility function, it is thus difficult to fit with linear regression because of the extremal curvation in the utility function, unless constrained locally. Due to the S-shape behaviour of the utility from assumption 1.3.1, these basis functions might produce inaccurate results. Besides, payoff and utility that are highly non-linear, abruptly changing or non-continuous can be harder for the LSMC algorithm to handle, by Zhang et al. (2019). Increase the complexity of the basis function might be helpful to improve the accuracy, but it also requires an increase of the sample paths with a large computational cost.

Andreasson & Shevchenko (2019) gives a possible solution to a similar problem with increasing, monotonic and concave utility function by transforming the utility and try to avoid the re-transform bias. We try to extend this method to the S-shaped utility.

The idea of the transformation is to reduce the non-linearity of the utility function, and the heteroskedastic, that is having different variances, of the fitted residuals. The least-squares regression will then be performed to the transformed value function.

Let the invertible transformation $T : \mathbb{R} \to \mathbb{R}$ and the inverse $T^{-1} : \mathbb{R} \to \mathbb{R}$, such that $T^{-1}(T(x)) = x$. Then the state variable under the transformation still depends on the control. We define $\mathbf{L}(X_t, \Pi_t)$ be a basis vector function and $\mathbf{\Lambda}_t$ is the corresponding coefficients vector. Then as described, the value function with transformed utility is approximated as

$$\mathbb{E}\left[T\left(V_{t_{i+1}}\left(X_{t_{i+1}}\right)\right) \mid X_{t_i}; \Pi_{t_i}\right] = \mathbf{\Lambda}'_{t_i} \mathbf{L}\left(X_{t_i}, \Pi_{t_i}\right).$$

By the ordinary linear regression, with M independent paths of the state process and the corresponding realised control variables, we assume that

$$T\left(V_{t_{i+1}}\left(X^m_{t_{i+1}}\right)\right) = \mathbf{\Lambda}'_{t_i} \mathbf{L}\left(X^m_{t_i}, \Pi_{t_i}\right) + \epsilon^m_{t_i},$$
$$\text{where } \epsilon^m_{t_i} \overset{iid}{\sim} F_{t_i}(\cdot), \quad \mathbb{E}\left[\epsilon^m_{t_i}\right] = 0, \quad \text{var}\left[\epsilon^m_{t_i}\right] = \sigma^2_{t_i}, \quad m = 1, \ldots, M$$

for some distribution $F_{t_i}(\epsilon_{t_i})$ of ϵ_{t_i}. The best linear unbiased estimator of $\mathbf{\Lambda}_{t_i}$ is then given as

$$\widehat{\mathbf{\Lambda}}_{t_i} = \arg\min_{\mathbf{\Lambda}_{t_i}} \sum_{m=1}^{M} \left[T\left(V_{t_{i+1}}\left(X_{t_{i+1}}^m \right) \right) - \mathbf{\Lambda}_{t_i}' \mathbf{L}\left(X_{t_i}^m, \Pi_{t_i}^m \right) \right]^2.$$

Note that $\widehat{\mathbf{\Lambda}}_{t_i}$ is consistent and asymptotically normally distributed, and it will be the maximum likelihood estimator if the distribution $F_{t_i}(\epsilon_{t_i})$ is normal.

After the transformation and the approximation, we then try to re-transform the estimated function into the original scale, that is having $\Phi_{t_i}(X_{t_i}(\Pi), \Pi_t)$ as the form

$$\begin{aligned} \Phi_{t_i}(X_{t_i}(\Pi), \Pi_t) &:= T^B\left(\mathbf{\Lambda}_{t_i}' \mathbf{L}\left(X_{t_i}, \Pi_{t_i} \right) \right) \\ &= \int T^{-1}\left(\mathbf{\Lambda}_{t_i}' \mathbf{L}\left(X_{t_i}, \Pi_{t_i} \right) + \epsilon_{t_i} \right) dF_{t_i}(\epsilon_{t_i}). \end{aligned} \tag{2.2.1}$$

A simple idea is to let $T^B = T^{-1}$. However, even the true $\mathbf{\Lambda}$ is given, by the Jansen's inequality, we will still have $\mathbb{E}[U(\cdot)] \leq U(\mathbb{E}[\cdot])$ in the concave part of the utility function and $\mathbb{E}[U(\cdot)] \geq U(\mathbb{E}[\cdot])$ in the convex part, since in this process we estimate the state variable first then perform the utility which should be done in reverse direction by equation (1.3.1). Hence letting $T^B = T^{-1}$ will result in neither unbiased nor consistent results. Another issue is that unless the distribution of ϵ_{t_i} is known, equation (2.2.1) is both analytically and numerically unsolvable. Thus we have to estimate the distribution of the residuals as well as reduce the bias the re-transformation might causes.

2.3 Smearing estimate with heteroskedasticity

Duan (1983) produced a non-parametric method, the smearing estimate, to deal with the re-transformation problem as described in section 2.2. It's an effective consistent estimate of the expected response on the original scale after a linear regression on a transformed scale. Duan (1983) described it as a type of low-premium insurance against departures from the assumptions of the parameter distribution.

For symbol simplification, in this section, we denote the original observations of the value function at given time t as $Y^m, m = 1, \ldots, M$ and the corresponding transformed value as $\eta^m, m = 1, \ldots, M$ such that $\eta^m = T(Y^m), Y^m = T^B(\eta^m)$, i.e. $T^B = T^{-1}$. Assume that both T and T^B are monotonic and continuously differentiable. Then the linear regression performed on the transformed observations can be denoted as

$$\eta^m = \mathbf{\Lambda}'\mathbf{L}^m + \epsilon^m, \quad \epsilon^m \overset{\text{i.i.d}}{\sim} F(\cdot), \quad \mathbb{E}[\epsilon^m] = 0, \quad \text{var}[\epsilon^m] = \sigma^2,$$

where $\mathbf{\Lambda}$ is the coefficient vector , $\mathbf{L}^m$ is the vector of chosen basis based on the observed value and ϵ^m is the corresponding independent and identically distributed residuals that follows some distribution $F(\cdot)$ with zero mean and finite variance. Note that $F(\cdot)$ can be unknown as long as it has zero mean and constant variance.

By Jensen's inequality, if we perform the re-transformation T^{-1} to the prediction of the transformed value, i.e. letting $T^B = T^{-1}$, the result would be inaccurate since $\mathbb{E}[Y] \leq T^{-1}(\mathbb{E}[\mathbf{\Lambda}'\mathbf{L} + \epsilon])$ if T^{-1} is concave and $\mathbb{E}[Y] \geq T^{-1}(\mathbb{E}[\mathbf{\Lambda}'\mathbf{L} + \epsilon])$ if T^{-1} is convex.

Duan (1983) suggest that instead, we can have the approximation in the form of

$$\begin{aligned} \mathbb{E}[Y] &= \mathbb{E}\left[T^{-1}(\mathbf{\Lambda}'\mathbf{L} + \epsilon) \right] \\ &= \int T^{-1}(\mathbf{\Lambda}'\mathbf{L} + \epsilon)\, dF(\epsilon) \end{aligned}$$

after the estimation of the coefficient $\mathbf{\Lambda}$ by using the empirical distribution function (edf) of ϵ where the edf is of the form

$$\widehat{F}_M(e) = \frac{1}{M} \sum_{m=1}^{M} \mathbb{1}\{\widehat{\epsilon}^m \leq e\}$$

with the indicator function $\mathbb{1}$ that equals 1 if $\widehat{\epsilon}^m \leq e$ and 0 otherwise. Then the estimated

expectation of Y is given by

$$\begin{aligned}\widehat{\mathbb{E}}[Y] &= \int T^{-1}\left(\hat{\mathbf{\Lambda}}'\mathbf{L}+\epsilon\right) d\widehat{F}_M(\epsilon) \\ &= \frac{1}{M}\sum_{m=1}^{M} T^{-1}\left(\hat{\mathbf{\Lambda}}'\mathbf{L}+\hat{\epsilon}^m\right),\end{aligned}$$

where

$$\hat{\epsilon}^m = \eta^m - \hat{\mathbf{\Lambda}}'\mathbf{L}^m.$$

Notice that in Duan (1983) the variance of the residual is assumed to be constant, but in our model, as the state variable is affected by the control variable, heteroskedasticity is present in the regression. Hence we need to adjust the estimated residual.

Since the variance is not constant, we assume that $\text{var}[\epsilon^m] = \sigma^2 C(\mathbf{L}^m)$ for some new basis function $C(\mathbf{L}^m)$. We adopt the method from Harvey (1976) to estimate function $C(\mathbf{L}^m)$ that causes the heteroskedasticity. To avoid negative value, we let $C(\mathbf{L}^m) = \exp(\mathcal{L}'\mathbf{L}^m)$, where $\mathcal{L} = \mathcal{L}_0, \mathcal{L}_1, \ldots, \mathcal{L}_K$ is another regression coefficient vector, Then the residual is of the form

$$\epsilon^{m\,2} = \sigma^2 C(\mathbf{L}^m) v = \sigma^2 e^{\mathcal{L}'\mathbf{L}^m} v^2, \quad \mathbb{E}[v] = 0, \mathbb{E}\left[v^2\right] = 1.$$

Hence

$$\ln\left(\epsilon^{m\,2}\right) = a + \mathcal{L}_1 L_1^m + \ldots + \mathcal{L}_K L_K^m + \ln v^2$$

with $a = \ln\left(\sigma^2\right) + \mathcal{L}_0$. Then at given time t, the conditional variance ϵ^m can be estimated as

$$\widehat{\text{var}}\left[\hat{\epsilon}^m \mid X, \Pi\right] = \left[\mathcal{H}\left(\hat{\sigma}^2 \exp\left(\hat{\mathcal{L}}'\boldsymbol{L}\right)\right)\right]^2$$

with some positive function $\mathcal{H}(\cdot)$. Then by Zhou et al. (2008), we can extend the smearing estimate to the heteroskedasticity cases and estimate the re-transform function at time t as

$$\hat{T}^B\left(\hat{\Lambda}_t'\mathbf{L}\left(X_t, \Pi_t\right)\right) = \frac{1}{M}\sum_{m=1}^{M} T^{-1}\left(\begin{array}{l}\hat{\mathbf{\Lambda}}'\mathbf{L}\left(X_t, \Pi_t\right) + \mathcal{H}\left(\hat{\sigma}^2 \exp\left(\hat{\mathcal{L}}'\boldsymbol{L}(X_t, \Pi_t)\right)\right) \\ \qquad \dfrac{\hat{\epsilon}_t^m}{\mathcal{H}\left(\hat{\sigma}^2 \exp\left(\hat{\mathcal{L}}'\boldsymbol{L}(X_t^m, \Pi_t^m)\right)\right)}\end{array}\right).$$

Remark 2.3.1. If the state is not heteroskedasticity, then we can simplify the estimation of the re-transform function as

$$\hat{T}^B\left(\hat{\Lambda}_t'\mathbf{L}\left(X_t, \Pi_t\right)\right) = \frac{1}{M}\sum_{m=1}^{M} T^{-1}\left(\hat{\mathbf{\Lambda}}'\mathbf{L}\left(X_t, \Pi_t\right) + \hat{\epsilon}_t^m\right).$$

Note that we don't require the utility function to be differentiable or continuous as long as the transformation function can reduce the non-linearity or heteroskedasticity can be found. One can use generalized linear model (GLM) without the transformation to perform the estimation to the value function, which can also deal with the heteroskedasticity by a link function. However, by Baser (2007), the result from GLM might be imprecise if the distribution $F(\cdot)$ is mis-specified. For the flexibility of the algorithm, we prefer the smearing estimate and adjust the re-transformation function from heteroskedasticity.

2.4 The basic LSMC method with exogenous state

In this section, we provide a brief introduction to the basic Least-Squares Monte Carlo method with exogenous states as shown in Algorithm 1. In the basic algorithm, the state is not affected by the control, but we assume that the utility function hence the value function, the transformation and re-transformation function does.

A general LSMC method contains two parts, one forward simulation process and one backward optimisation process. If the state X_{t_i} is exogenous, then M random paths can be generated as

$$X_{t_{i+1}}^m = \mathcal{T}_{t_i}\left(X_{t_i}, Z_{t_{i+1}}\right), \quad m = 1, \ldots, M$$

for time $t_i,\ i = 0, \ldots, n$. Then the problem is solved by a backward recursion starting from time $t_n = T$. From time $t_i = T - \boldsymbol{\Delta}$, we find the optimal control for each t_i by performing the regression of the value function at time t_{i+1} over the state variable at time t_i. Once the optimal control is found, we update the value function with the optimised control then repeat the process till time $t_0 = 0$.

Algorithm 1: The basic LSMC method with exgenous state

Data: Looping period N, number of sample paths M, initial capital x_0, and other value of variables to determine the behaviour of the state and the constraint

Result: Output estimated maximised utility at time $t_0 = 0$ as V_{t_0}

[forward simulation]

for $i = 0$ **to** n **do**
  for $m = 0$ **to** M **do**
    if $i = 0$ **then**
      let $X_{t_i}^m$ be x_0
    else
      let $X_{t_i}^m$ be $\mathcal{T}_{t_{i-1}}\left(X_{t_{i-1}}, Z_{t_i}\right)$
    end
  end
end

[backward simulation]

for $i = n$ **to** 0 **do**
  if $i = n$ **then**
    let $\widehat{V}_{t_i}\left(\boldsymbol{X}_{t_i}\right)$ be $U(\boldsymbol{X}_{t_i})$
  else
    estimate $\widehat{\Lambda}_t$ as
    $$\arg\min_{\boldsymbol{\Lambda}_{t_i}} \sum_{m=1}^{M} \left[T\left(V_{t_{i+1}}\left(X_{t_{i+1}}^m, \Pi_{t_{i+1}}\right)\right) - \boldsymbol{\Lambda}_{t_i}' \mathbf{L}\left(X_{t_i}^m\right)\right]^2;$$
    find the re-transform function $T^B(\boldsymbol{\Lambda}_{t_i}' \mathbf{L}(X_{t_i}))$;
    let $\widehat{\Phi}_{t_i}\left(\boldsymbol{X}_{t_i}, \boldsymbol{\Pi}_{t_i}\right)$ be $T^B(\boldsymbol{\Lambda}_{t_i}' \mathbf{L}(\boldsymbol{X}_{t_i}), \boldsymbol{\Pi}_{t_i})$;
    for $m = 1$ **to** M **do**
      find the optimal control $\Pi_{t_i}^*\left(X_{t_i}^m\right)$ as
      $$\arg\sup_{\Pi_t \in \mathcal{A}(K)} \left\{\widehat{\Phi}_{t_i}\left(X_{t_i}^m, \Pi_{t_i}\right)\right\};$$
      let $\widehat{V}_{t_i}\left(X_{t_i}^m, \Pi_{t_i}\right)$ be $\widehat{\Phi}_{t_i}\left(X_{t_i}^m, \Pi_{t_i}^*\right)$;
    end
  end
end

store value $\hat{V}_{t_0}$

One typical usage of the basic LSMC method is to estimate the price of the American option. These options can be exercised at any time before and at maturity, which is more difficult to price than European options as one has to determine the exercise time of the option. Since utility functions are not used for the pricing problem, transformation of the value function is not required if we perform the LSMC method. To illustrate, let's consider the American put option with two underlings with payoff $(K - S_1(\tau) - S_2(\tau))^+$ where K is the strike price, and S_1, S_2 are two corresponding stocks. This kind of option is called the American spread put option. We assume that the two stocks satisfy

$$\begin{aligned} dS_1(t) &= rS_1(t)dt + \sigma_1 S_1(t)dW_1(t), \\ dS_2(t) &= rS_2(t)dt + \sigma_2 S_2(t)dW_2(t), \\ dW_1(t)dW_2(t) &= \rho dt, \end{aligned}$$

where W_1 and W_2 are two standard Brownian motions with correlation ρ under risk neutral probability $\mathbb{Q}$. By Hu (2013), the basis function is taken as $\boldsymbol{L}(S_1, S_2) = (1, S_1, S_2, S_1^2, S_2^2)$, and the continuation value is approximated as $\hat{V}_C = \boldsymbol{L}\left(s_1, s_2\right)\boldsymbol{\Lambda}_{t_i}'$, for $i = 0, 1, \cdots, n-1$ with

$\mathbf{\Lambda}_{t_i} = (\Lambda_{i1}, \Lambda i2, \cdots, \Lambda iJ)$ where $J = 5$. By simple algebra, we can estimate $\mathbf{\Lambda}_{t_i}$ as $\tilde{\mathbf{\Lambda}}_i = \widetilde{\lambda}_L^{-1}\widetilde{\lambda}_{LV}$ with

$$\widetilde{\lambda}_L = \frac{1}{M}\sum_{m=1}^{M} \boldsymbol{L}\left(S_1^m(t_i), S_2^m(t_i)\right)\left[\boldsymbol{L}\left(S_1^m(t_i), S_2^m(t_i)\right)\right]^T,$$
$$\widetilde{\lambda}_{LV} = \frac{1}{M}\sum_{n=1}^{M} \boldsymbol{L}\left(S_1^m(t_i), S_2^m(t_i)\right) V_{t_{i+1}}\left(S_1^m(t_{i+1}), S_2^m(t_{i+1})\right),$$

where M denoted the number of sample path and V_{t_i} is the payoff at time t_i. Then by the LSMC method, we can simulate the price of the American put option with two assets with Algorithm 2.

Algorithm 2: The LSMC mehtod for American put option with two underlyings

Data: Initial stock prices $\boldsymbol{S_0}$, strike price K, interest rate r, correlation ρ, volatilises $\boldsymbol{\sigma}$, time periods N, maturity T, sample size M, payoff at maturity $\boldsymbol{h} = (h_1, h_2, \cdots, h_M)$

Result: Output estimated payoff at time $t_0 = 0$ as V_{t_0}

Generate M different paths of the underlying process:
$\{S_1^m(t_1), S_1^m(t_2)\cdots, S_1^m(t_n)\}$ and $\{S_2^m(t_1), S_2^m(t_2)\cdots, S_2^m(t_n)\}$ for $m = 1, 2, \cdots M$;
at maturity, set $\tilde{V}_n = \boldsymbol{h}$;
while *time period is less than n, let* $i = n-1, \cdots, 2, 1$ **do**
  compute $\tilde{\mathbf{\Lambda}}_{t_i} = \widetilde{\lambda}_L^{-1}\widetilde{\lambda}_{LV}$;
  compute $\tilde{c}_{t_i} = \boldsymbol{L}\tilde{\mathbf{\Lambda}}'_{t_i}$ for all paths;
  compute $\tilde{V}_{t_i}$ for all paths as
  if $h_{t_i} > \tilde{c}_{t_i}$ **then**
    let $\tilde{V}_{t_i}$ be h_{t_i}
  else
    let $\tilde{V}_{t_i}$ be $\tilde{V}_{t_{i+1}}$
  end
end
set $\tilde{V}_{t_0}^{(m)} = h_{t_i}$, where $t_i = \min\{t_i \in \{t_1, \cdots, t_n\} : h_{t_i} \geq \tilde{c}_{t_i}\}$ for all paths;
store estimated option price $\tilde{V}_{t_0} = \frac{1}{M}\sum_{m=1}^{M} \tilde{v}_0^{(m)}$

For empirical exercise, we let the initial stock price $\boldsymbol{S_0} = (100, 100)$, strike price $K = 200$, interest rate $r = 006$, correlation of the two Brownian Motion $\rho = 0.5$, volatilities $\boldsymbol{\sigma} = (0.4, 0.2)$ with maturity $T = 1$. Table 2.2 shows the result with time periods $n \in \{100, 1000, 10000\}$ and $M = 1000$ paths and figure 2.1 shows the simulated option value with respect to strike price $K \in [150, 200]$ without changing other parameters. Noticing that all the payoffs are around 4.5, though the comparison with the exact value from the PDE solution is not included, it's reasonable to expect the value at time $t = 0$ to be around this value.

Time steps	$N = 100$	$N = 1000$	$N = 10000$
LSMC Simulation	4.4754	4.5586	4.4215

Table 2.2: Put prices at time $t = 0$ from the LSMC simulation method under 1000 paths with different time steps n for the American put option with two underlying assets ($\boldsymbol{S_0} = (100, 100), K = 200, \boldsymbol{\sigma} = (0.4, 0.2), r = 0.06, \rho = 0.5$ and $T = 1$).

2.5 The LSMC method with endogenous state

Now we extend the basic LSMC algorithm presented in Section 2.4 to endogenous cases. We adopt the method from Kharroubi et al. (2014) with the control randomisation technique. The algorithm is also based on a forward simulation and a backward optimisation, where the state variable is affected by both the random control and the perturbation term in the forward simulation. The

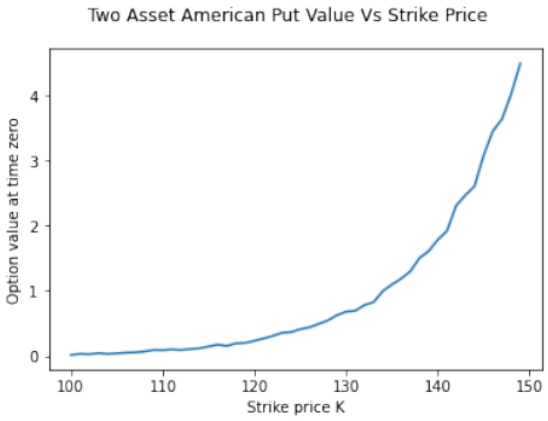

Figure 2.1: Option value at time $t = 0$ with respect to strike price $K = 200$.

basis function of the regression to the conditional expectation is then based on the state and the control variables.

2.5.1 Forward simulation

The forward simulation with endogenous states is more delicate than with the exogenous states. The main goal of the forward simulation is to generate large enough data and hence enough information to estimate the conditional expectation of the state and the control.

If we perform the forward simulation process that present in Algorithm 1, then random control $\widetilde{\Pi}^m_{t_i}$ is required on each simulated path $X^m_{t_i}, t = 0, \ldots, n$. However, it will cause a problem if the value of the optimal control $\Pi^*_{t_i}$ takes a value that close to the lower or upper bound in the admissible set $\mathcal{A}(K)$. If the random control is assumed to follow a uniform distribution, then the simulated state process might lay in a sub-domain that differs from the one the optimal control is used. On the other hand, if the range of the optimal control is known, then a more appropriate distribution that lives in the same range can be applied to improve the simulation of the random control as more samples would lay in the same sub-domain as the optimal control applied. Note that both of the two issues make it more difficult to perform the regression as the number of state sample paths in the first issue and the control process in the second issue might not be large enough in the full expected domain.

Hence, we try to figure out a more appropriate approach to simulate the control and the state process in the full domain to have a better regression result. We achieve this by simulating random states $\widetilde{X}_{t_i}$ that is independent of the controls and states over time $t_{i-1}, \ldots, t_0$ where $\widetilde{X}_{t_i} = \mathcal{T}_{t_{i-1}}\left(X_{t_{i-1}}, \Pi_{t_{i-1}}, z_{t_i}\right)$ with X_{t_i} being an independent random sample from the full state domain. Note that if X_{t_i} can be simulated by the function $\mathcal{T}(\cdot)$ for all $i = 1, \ldots, n$, then so is $\widetilde{X}_{t_i}$. Since each X_{t_i} is independent of the previous state, it can spread over the full domain at each time period, allowing the algorithm to explore the space better.

Algorithm 3 shows the updated forward simulation of the LSMC method.

Note that for independently sampling X_{t_i}, $\widetilde{\Pi}_{t_i}$ and $z^m_{t_{i+1}}$ in Algorithm 3, distribution for $z_{t_{i+1}}$ should be model specified while the other two can be flexible as long as they are appropriate to the specific problem.

2.5.2 Backward simulation

Kharroubi et al. (2014) suggest two different control randomisation algorithm to estimate the conditional expectation. One is a policy function iteration that uses the realised value to update the value function with

$$\widehat{V}_{t_i}\left(X_{t_i}\right) = \widehat{V}_{t_i}\left(X_{t_i}(\Pi^*_{t_i})\right),$$

Algorithm 3: The updated forward simulation

Data: Looping period N, number of sample paths M, initial capital x_0, and other value of variables to determine the behaviour of the state and the constraint

Result: Output simulated state process $\widetilde{X}$, X and the control process $\tilde{\Pi}$

[forward simulation]

1 **for** $i = 0$ **to** $n-1$ **do**
2 **for** $m = 1$ **to** M **do**
3 let $X_{t_i}^m$ be independent random sample from $\mathcal{X}$;
4 let $\tilde{\Pi}_{t_i}^m$ be independent random sample from $\mathcal{A}(K)$;
5 let $z_{t_{i+1}}^m$ be independent random sample from $\mathcal{Z}$;
6 let $\widetilde{X}_{t_{i+1}}^m$ be $\mathcal{T}_{t_i}\left(X_{t_i}^m, \Pi_{t_i}^m, z_{t_{i+1}}^m\right)$
7 **end**
8 **end**
9 store vector $\widetilde{X}$, X and $\tilde{\Pi}$

and the other one is a value function iteration which uses the regression result with

$$\widehat{V}_{t_i}\left(X_{t_i}\right) = \widehat{\Phi}_{t_i}\left(X_{t_i}.\Pi_{t_i}^*\left(X_{t_i}\right)\right),$$

The first iteration method requires re-calculating the sample path from time t_{i+1} to time t_n at every time t_i once the optimal value is calculated as the optimal control will affect the future state. However, this effect is estimated in the value function iteration with $\widehat{\Phi}_{t_i}\left(X_{t_i}, \Pi_{t_i}\right)$. Denault et al. (2017) proved that there is no difference between the two iteration methods with exogenous states. Though the policy function iteration is more computational complex, it is more accurate with fewer regression errors over time and more suitable for problems that tend to produce regression error as the number of time periods increases.

We provide the algorithms with these two iteration methods separately. In both algorithms, the estimate of the conditional expectation $\hat{\Phi}_{t_i}(\cdot)$ at time t_{i+1} is performed with a regression function, then the optimal control is found by maximising the approximated value function.

As shown in Algorithm 4, in the policy function iteration, the sample state process from time t_{i+1} to time t_n is updated once the optimal control at time t_i is solved, then the corresponding value function for the realised process is stored for the next iteration. Note that at terminal time t_n, no decision is taken and $\widetilde{X}_{t_n} = X_{t_n}$. The loop from line 13 onwards updates the forward simulation at each backward step with optimal control, which is crucial to multi-period stochastic control problems with utility functions, unless the basis function holds true over the whole period. It also implies that the algorithm uses the realised value function but not the regression result to update the value function. As the time horizon increases, this loop significantly improves the accuracy of the approximation and reduces the risk of solution blow-up by restricting the accumulation of regression errors. Note that in the loop of line 13, the optimal control Π_t^* has to be resolved at each time period, making the algorithm computationally more costly. Thus we choose to store the optimal control from each state sample and use it for every corresponding evaluation time t, which faster the algorithm significantly but also brings some acceptable simulation error.

Algorithm 5 updates the value function with regression results but not realised value, and it also does not update the forward simulation at each looping period. This algorithm is computationally simpler and hence faster but might stack regression errors in the value function.

Note that since the initial value at time $t_0 = 0$ of X_{t_0} is given, $\widetilde{X}_{t_0}^m$ is of the same value for all $m = 1, \ldots, M$, hence at the last loop for $i = 0$, we can replace line 9 in algorithm 4 and 9 in algorithm 5 with $\widehat{X}_{T_0}^m := x_0$.

It's worth mentioning that this extension is computational heavy due to the regression and optimisation during each loop. Since we will at least have $M * n$ optimisations and n regressions at one go and for stable purpose, from our experience, normally we require to set $M = 5000$ and $n = 20$ for time horizon $T = 1$ as minimum sample size to have an acceptable result which leads to $100,000$ optimisations when performing the algorithm. Even we parallel the computation, it takes hours to get the result with $200,000$ optimisations on a normal family laptop with 6 cores by R.

Algorithm 4: Backward solution with policy function iteration

Data: Looping period N, number of sample paths M, simulated $\widetilde{X}$, X and $\tilde{\Pi}$ from forward simulation

Result: Output estimated maximised utility at time $t_0 = 0$ as V_{t_0}

for $i = n$ **to** 0 **do**
  if $i = n$ **then**
    let $\widehat{V}_{t_i}\left(\widetilde{\boldsymbol{X}}_t\right)$ be $U(\widetilde{\boldsymbol{X}}_t)$
  else
    estimate $\widehat{\Lambda}_t$ as
      $\arg\min_{\boldsymbol{\Lambda}_{t_i}} \sum_{m=1}^{M}\left[T\left(V_{t_{i+1}}\left(\widetilde{X}^m_{t_{i+1}}\right)\right) - \boldsymbol{\Lambda}'_{t_i}\mathbf{L}\left(X^m_{t_i}, \widetilde{\boldsymbol{\Pi}}^m_{t_i}\right)\right]^2$;
    find the re-transform function $T^B(\boldsymbol{\Lambda}'_{t_i}\mathbf{L}(X_{t_i}, \widetilde{\boldsymbol{\Pi}}_{t_i}))$;
    let $\widehat{\Phi}_{t_i}\left(\boldsymbol{X}_{t_i}, \widetilde{\boldsymbol{\Pi}}_{t_i}\right)$ be $T^B(\boldsymbol{\Lambda}'_{t_i}\mathbf{L}(\boldsymbol{X}_{t_i}, \widetilde{\boldsymbol{\Pi}}_{t_i}))$;
    for $m = 1$ **to** M **do**
      let $\widehat{X}^m_{t_i}$ be $\widetilde{X}^m_{t_i}$;
      find the optimal control $\Pi^*_{t_i}\left(\widehat{X}^m_{t_i}\right)$ as
        $\arg\sup_{\Pi_t \in \mathcal{A}(K)}\left\{\widehat{\Phi}_{t_i}\left(\widehat{X}^m_{t_i}, \Pi_{t_i}\right)\right\}$;
      let $\widehat{V}_{t_i}\left(\widehat{X}^m_{t_i}\right)$ be $U\left(\widehat{X}^m_{t_i}\left(\Pi^*_{t_i}\right)\right)$;
      let $\widehat{X}^m_{ti+1}$ be $\mathcal{T}_{t_i}\left(\widehat{X}^m_{t_i}, \Pi^*_{t_i}\left(\widehat{X}^m_{t_i}\right), z^m_{t_{i+1}}\right)$;
      for $j = i+1$ **to** $n-1$ **do**
        let $\widehat{X}^m_{t_{j+1}}$ be $\mathcal{T}_{t_j}\left(\widehat{X}^m_{t_j}, \Pi^*_{t_j}\left(\widehat{X}^m_{t_j}\right), z^m_{t_{j+1}}\right)$;
      end
      let $\hat{V}_{t_i}\left(\hat{X}^m_{t_i}\right)$ be $\hat{V}_{t_n}\left(\hat{X}^m_{t_n}(\Pi^*_{t_n})\right)$;
    end
  end
end
store value $\hat{V}_{t_0}$

2.6 Accuracy of solution

In this section, we examine the impacts of the smearing estimate on the accuracy of the LSMC simulation. Though the analytical solution to our model defined as equation (1.3.1) does not exist at the moment, which makes it hard to examine the exact accuracy, we can still speculate on the accuracy of our approach by the solution of another similar problem.

For simplification, we consider the model from Denault et al. (2017) which is based on the Constant Relative Risk Aversion (CRRA) utility with optimal consumption and risky allocation. The value of the model parameter is the same as the one that causing the problem in Denault et al. (2017). The basis functions are ordinary polynomials up to 4-th order in state and control with mixed terms. The CRRA utility is defined as $U(x) = x^\gamma/\gamma$, and the transformation function is defined as

$$T(x) = \ln\left[(\gamma x)^{1/\gamma}\right].$$

We consider a simple model that the trader consumes a proportion of wealth α_{t_i}, and chooses to allocate a proportion $\delta_{t_i} \in [0,1]$ of remaining into the risky asset with return Z_{t_i} and invest the rest into the risk-free bond with constant rate r. Let Z follows a normal distribution with mean μ and variance σ^2, then the transition function is approximately

$$X_{t_{i+1}} = \mathcal{T}_{t_i}\left(X_{t_i}, \pi_{t_i}, Z_{t_{i+1}}\right) := X_{t_i}\left(1-\alpha_{t_i}\right)e^{\delta_{t_i}Z_{t_{i+1}} + \left(1-\delta_{t_i}\right)r},$$

when the return is small. By Andreasson & Shevchenko (2019), the smearing estimation method with heteroskedasticity considers the effect of the perturbation term when performing the re-

Algorithm 5: Backward solution with value function iteration

Data: Looping period N, number of sample paths M, simulated $\widetilde{X}$, X and $\tilde{\Pi}$ from forward simulation

Result: Output estimated maximised utility at time $t_0 = 0$ as V_{t_0}

for $i = n$ **to** 0 **do**
  if $i = n$ **then**
    let $\widehat{V}_{t_i}\left(\widetilde{\boldsymbol{X}}_t\right)$ be $U(\widetilde{\boldsymbol{X}}_t)$
  else
    estimate $\widehat{\Lambda}_t$ as
      $\arg\min_{\boldsymbol{\Lambda}_{t_i}} \sum_{m=1}^{M}\left[T\left(V_{t_{i+1}}\left(\widetilde{X}^m_{t_{i+1}}\right)\right) - \boldsymbol{\Lambda}'_{t_i}\mathbf{L}\left(X^m_{t_i}, \widetilde{\boldsymbol{\Pi}}^m_{t_i}\right)\right]^2$;
    find the re-transform function $T^B(\boldsymbol{\Lambda}'_{t_i}\mathbf{L}(X_{t_i}, \widetilde{\boldsymbol{\Pi}}_{t_i}))$;
    let $\widehat{\Phi}_{t_i}\left(\boldsymbol{X}_{t_i}, \widetilde{\boldsymbol{\Pi}}_{t_i}\right)$ be $T^B(\boldsymbol{\Lambda}'_{t_i}\mathbf{L}(\boldsymbol{X}_{t_i}, \widetilde{\boldsymbol{\Pi}}_{t_i}))$;
    for $m = 1$ **to** M **do**
      let $\widehat{X}^m_{t_i}$ be $\widetilde{X}^m_{t_i}$;
      find the optimal control $\Pi^*_{t_i}\left(\widehat{X}^m_{t_i}\right)$ as
        $\arg\sup_{\Pi_t \in \mathcal{A}(K)}\left\{\widehat{\Phi}_{t_i}\left(\widehat{X}^m_{t_i}, \Pi_{t_i}\right)\right\}$;
      let $\hat{V}_{t_i}\left(\hat{X}^m_{t_i}\right)$ be $\widehat{\Phi}_{t_i}\left(\widehat{X}^m_{t_i}, \Pi^*_{t_i}\left(\widehat{X}^m_{t_i}\right)\right)$;
    end
  end
end
store value $\hat{V}_{t_0}$

transformation and leads to an unbiased solution if the value function is of the form

$$V_0(x) = \sup_{\Pi} \mathbb{E}\left[\beta^n R_{t_n}\left(X_{t_n}(\Pi)\right) + \sum_{i=0}^{n-1}\beta^i R_{t_i}\left(X_{t_i}(\Pi), \Pi_{t_i}\right) \mid X_{t_0}(\Pi) = x; \Pi\right], \tag{2.6.1}$$

leading to the optimisation problem

$$V_{t_i}(x) = \sup_{\Pi_{t_i}}\left\{R_{t_i}(x, \Pi_t) + \mathbb{E}\left[\beta V_{t_{i+1}}\left(X_{t_{i+1}}(\Pi)\right) \mid X_{t_i}(\Pi) = x; \Pi_{t_i}\right]\right\}, i = n-1, \ldots, 0$$
$$V_{t_n}(x) = R_{t_n}(x),$$

where R_{t_n} and R_{t_i} are some reward functions and β is the time discount factor over a time step. The optimal consumption can then be solved as

$$\alpha_{t_i} = \begin{cases} 1, & \text{if } i = n \\ \left(1 + \left(e^{\gamma\delta_{t_i}\mu + \gamma^2\delta^2_{t_i}\sigma^2/2 + \left(1-\delta_{t_i}\right)\gamma r}\alpha^{\gamma-1}_{t_{i+1}}\right)^{\frac{1}{1-\gamma}}\right)^{-1}, & \text{otherwise} \end{cases}, \tag{2.6.2}$$

with optimal risky allocation

$$\delta_{t_i} = \frac{r - \mu}{\gamma\sigma^2},$$

and the value function is

$$V_{t_i}\left(X_{t_i}\right) = \frac{\left(X_{t_i}\right)^\gamma}{\gamma}\left(\alpha_t\right)^{\gamma-1}.$$

Figure 2.2 shows the simulation result of the problem with and without re-transformation by the LSMC method. The terminal time T is set to be 9 with $n = 9$ with the mean of the perturbation term $\mu = 0.1$ and variance $\sigma = 0.2$. By letting $\gamma = -10$ and the risk-free rate be $r = 0.03$, with $M = 10000$ paths simulated, figure 2.2 shows that the optimal risky allocation blows up when performing the LSMC method without considering the heteroskedasticity while the one with transformation results in an acceptable simulation.

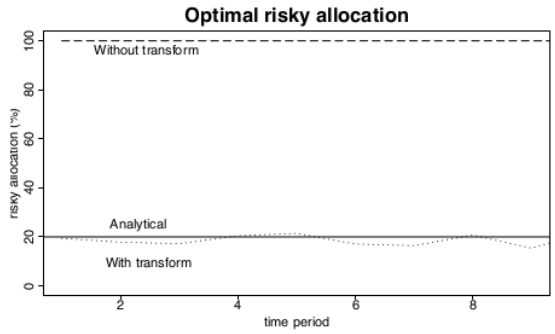

Figure 2.2: The simulated risky allocation by the LSMC method with and without transform and the exact numerical result.

Although equation (2.6.1) stands for a standard discrete dynamic programming problem, which slightly differs from problem (1.3.1), and the result from Andreasson & Shevchenko (2019) can only account for concave utility cases, we can still expect our algorithm to have a similar accuracy since an S-shaped function only contains a convex part with positive loss and concave part with positive gain. Moreover, problem (1.3.1) considers only the final gain at time t_n without other gains during the process at time $t_i, i = 1, \ldots, n-1$, which intuitively will reduce the regression error as the summation term that might accumulate the error is missing.

Chapter 3

Numerical results

This chapter uses the extended LSMC method with endogenous states to solve the portfolio optimisation problem presented as equation (1.3.1) with the two economic cases we consider in Chapter 1. The two utility functions that are taken is the same as in Armstrong et al. (2020), that is, the Kahneman & Tversky (2013) piecewise power function in the form of

$$U(x) = \begin{cases} x^{\beta_1}, & x \geq 0 \\ -k|x|^{\beta_2}, & x < 0 \end{cases} \tag{3.0.1}$$

as shown in figure 3.1 with $0 < \beta_1, \beta_2 < 1$ and $k > 0$, and the piecewise exponential function with the form

$$U(x) = \begin{cases} \phi_1 \left(1 - e^{-\gamma_1 x}\right), & x \geq 0 \\ \phi_2 \left(e^{\gamma_2 x} - 1\right), & x < 0 \end{cases} \tag{3.0.2}$$

as shown in figure 3.2 with $\phi_1, \phi_2, \gamma_1, \gamma_2 > 0$.

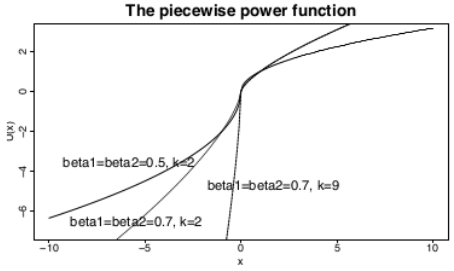

Figure 3.1: Piecewise power utility

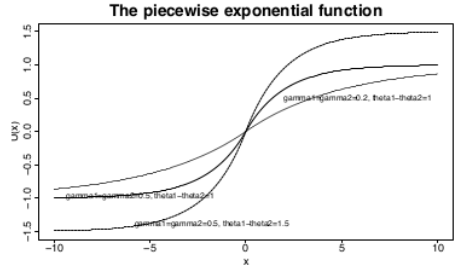

Figure 3.2: Piecewise exponential utility

Notice that we require the transformation function and the re-transformation function to be differentiable, but we do not require the utility function to be as well. Both the piecewise power utility and the piecewise exponential utility function are differentiable in $\mathbb{R}/\{0\}$. Since the transformation is taken to reduce the non-linearity or the heteroskedasticity of the value function, to reduce the non-linearity, we take the transformation function to be the inverse of the utility function $U(\cdot)^{-1}$ in domain $\mathbb{R}/(0-\delta, 0+\delta)$ for a small enough δ that less than 0.01, and be a polynomial $P(\cdot)$ up to order 2 in domain $(0-\delta, 0+\delta)$. The coefficient of the polynomial can be solved by equating both the value and the first-order differentiation of function $U(\cdot)^{-1}$ and $P(\cdot)$ at point $0-\delta$ and $0+\delta$. As such, the transformation function then follows the differentiable restriction, and the inverse can be solved numerically. The heteroskedasticity issue can be solved by letting the basis function in the regression be based on both the state and the control variable.

3.1 Simulation design

We assess the results of both economic cases described in Chapter 1 with basis functions as ordinary polynomials up to order 4 in both transformed state and control variables, including mixing terms. We found that using any polynomials with an order higher than 5 will cause over-fitting in both economic cases. We will analyse the performance of the LSMC output over a range of checking periods and time maturities. Additionally, we will apply the two utility functions as equations (3.0.1) and (3.3.1) to investigate the model properties in both economy cases.

In this study, we take the evaluation window $\mathbf{\Delta}$ to be 0.05 and compare the numerical solution of the value function at time $t_0 = 0$ under up to 10 equally spaced checking periods with terminal horizon $T = 1, 2, 3$. Further more, the models we explore are set with initial capital $x_0 = 1$, initial stock value $s_0 = 1$ and risk-free rate $r = 0.05$. The perturbation term is normal distribution with mean $\mu^J = \mu^B = 1$ and standard deviation $\sigma^J = \sigma^B = 0.25$. We will take the confidence level $\alpha \in \{0.05, 0.01\}$ with the exogenous limit of risk $R = 3$. Limited by the computational amount, the generated sample size M is set to be $10,000$.

Given that the utility function is taken as function $U(\cdot)$ with the transformation function $T(\cdot)$ and the re-transformation function $T^B(\cdot)$, the simulation for a single terminal horizon, single confidence level and single economy case is designed as follows

1. Simulate $M = 10,000$ samples of the state process $\widetilde{X}$, X and the control process $\tilde{\Pi}$ from algorithm 3

2. perform both backward solution algorithms 4 and 5 to get the result V_0^p and V_0^v

3. take the mean of the two values V_0^p and V_0^v to be the final result $V_{0,k}$

We repeat this process $K = 20$ times with different seeds to obtain a Monte Carlo estimate

$$V_0 = \frac{1}{K} \sum_{k=1}^{K} V_{0,k}.$$

In summary, a single extended LSMC experiment simulates multiple models for each T, R, α, and for every model simulating solutions of the problem (1.3.1) using two different backward simulation schemes, which undoubtedly has a very long rum-time. Hence, this is the reason why we chose to run an experiment with 20 models simulating $10,000$ points. This has enabled us to explore and compare all the combinations of different T, R and α and analyse the behaviour of both economy cases. Note that numeric integration also carries some errors that must be taken into account when analysing the performance of the models. Of course, increasing simulated samples and the size of the experiment would potentially reduce the Monte Carlo error.

The code for this simulation exercise can be found at Github.

3.2 Simulation results and discussions

In this section, we present the simulation results with some detailed discussions. A conclusion of the discussion will be provided in section 3.4. For a more visual presentation, most of the results will be presented by figures in this section and with tables if necessary. All the exact numerical results can be found in the tables attached in Appendix B.

3.2.1 The result with a jump process

As described in section 1.1, we do not take the Expected Shortfall into consideration in this economy cases due to the heavy computational amount. For both confidence level $\alpha = 0.05$ and $\alpha = 0.01$, we take coefficients of the piecewise power function and the piecewise exponential function as $\beta_1 = \beta_2 = 0.5$, $k = 2$, $\gamma_1 = \gamma_2 = 0.55$ and $\theta_1 = 1$, $\theta_2 = 2$ respectively. Figure 3.3 shows the result with piecewise power utility with 0.05 confidence level, and figure 3.4 shows the result with piecewise exponential utility.

Notice that all the results are decreasing in trend as the checking period increase. It is also no surprise to see that for a fixed checking period, the optimal value is positively related to the terminal horizon T.

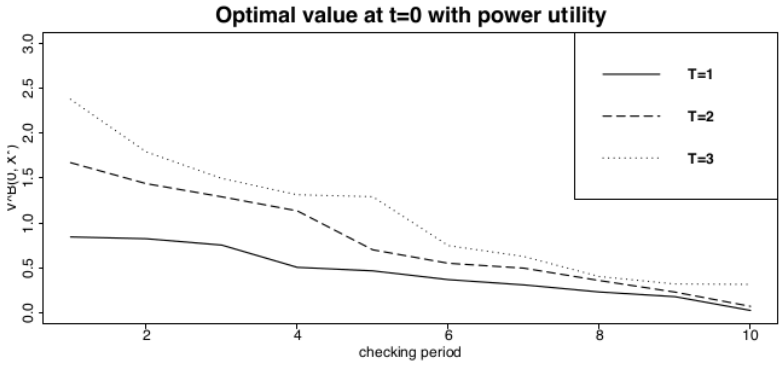

Figure 3.3: The simulated optimal result from 0.05 confidence level of the economy with jump process and piecewise power utility. The coefficient on the utility function is $\beta_1 = \beta_2 = 0.5$ and $k = 2$.

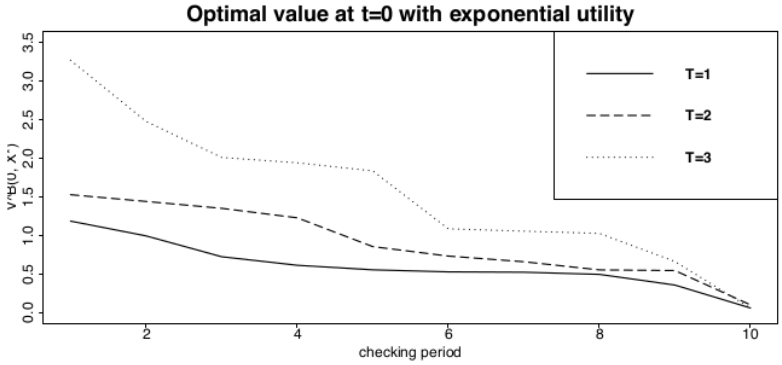

Figure 3.4: The simulated optimal result from 0.05 confidence level of the economy with jump process and piecewise exponential utility. The coefficient on the utility function is $\gamma_1 = \gamma_2 = 0.55$ and $\theta_1 = 1$, $\theta_2 = 2$.

One might be surprised that due to the result from Armstrong et al. (2020), the portfolio optimisation problem (1.3.1) will goes to infinity when there is no risk constraint applied, but it seems that even taking only one checking point at time $\tau = T/2$, the result is bounded efficiently. This is because in this economy case, the stock price only changes at time $t = T/2$ and $t = T$. Notice that $t = T/2$ is also the checking point for the portfolio manager, which will band the trader from investing infinitely many amounts into the stock to get an infinite payoff as his investment amount is limited. Though there is no constraint imposed in other evaluation time, the stock value also does not change, which keeps the trader from investing in the stock, preventing him from putting an extremely large amounts into the portfolio as only a limited payoff can be obtained from the risk-free asset. This can be supported by the simulation result of a single risk-free asset with a single checking point imposed at time $T/2$, resulting in optimised value $V_0 = 0.6195$ under the piecewise power utility, and $V_0 = 0.8578$ under the piecewise exponential utility. When we change this only checking point to any time not at $T/2$, the optimised solution goes to an incredibly large value. Furthermore, we would expect that the risk constraint is more effective to a stock larger total variation during the evaluation window if the variance of the stock is greater than zero, as the constraint we imposed for time not at $T/2$ can be regarded as a constraint over the combination of a risk-free bond and a special stock with fixed price.

In multi-checking-point cases, though for checking time $\tau \in \{2, 4, 6, 8, 10\}$, there is no constraint imposed at the time when the stock prices change, the two checking points that applied just before

and after time $T/2$ still bound the investment amount to a finite value since the losses at these two checking points is still non-constant and follows a shifted log-normal distribution.

Table 3.1 shows the simulated result under confidence level 0.01 without changing other parameters using piecewise power utility function, which still has a decreasing trend with the increased checking point amount. Notice that the outcomes are significantly larger than those from the 0.05 confidence level. This is probably because the piecewise power utility function is unbounded on the extremal losses and gains, which results in large expected utility when the constraint is imposed on a more extreme loss.

Time Horizon	$T=1$	$T=2$	$T=3$
1 checking point	7.9723×10^{9}	1.6829×10^{13}	3.5817×10^{18}
2 checking points	4.9276×10^{9}	2.8615×10^{10}	9.0724×10^{10}
3 checking points	5.1721×10^{8}	1.7918×10^{9}	8.2459×10^{10}
4 checking points	7.6527×10^{7}	3.1457×10^{8}	2.0380×10^{9}
5 checking points	2.8970×10^{7}	1.5445×10^{8}	8.0277×10^{8}
6 checking points	5.7796×10^{6}	1.7270×10^{7}	1.7368×10^{8}
7 checking points	2.2745×10^{6}	4.8567×10^{6}	3.6777×10^{6}
8 checking points	1.4715×10^{5}	2.7427×10^{5}	2.7886×10^{6}
9 checking points	1.5282×10^{2}	6.1647×10^{4}	1.2227×10^{5}
10 checking points	8.5393×10	1.2140×10^{2}	1.7256×10^{4}

Table 3.1: Simulated result under confidence level 0.01 using piecewise power utility function in the economy case with jump process.

Figure 3.5 shows the simulated result under confidence level 0.01 without changing other parameters using piecewise exponential utility function. Notice that the results under 0.01 confidence level are still higher than those under 0.05 level, which is because with 0.01 level, we only constraint on more extremal losses than the 0.05 one, resulting in a restricted maximum investment amount $\Pi^{J}_{max} = -7.122131$ in time horizon $[\frac{T}{2} - \delta, \frac{T}{2} + \delta] \cup [T - \delta, T]$ for any $\delta > 0$ which is higher than -11.54472 from the 0.05 level. Notice that with 10 checking points, the optimal solution for terminal horizon $T = 2$ and $T = 3$ is less than that from $T = 1$, which might be due to the numerical error as we tried with other seeds this situation did not appear again. With a large terminal horizon, we would expect larger errors in the numeric approximation of the true value as the number of simulated paths might not be large enough.

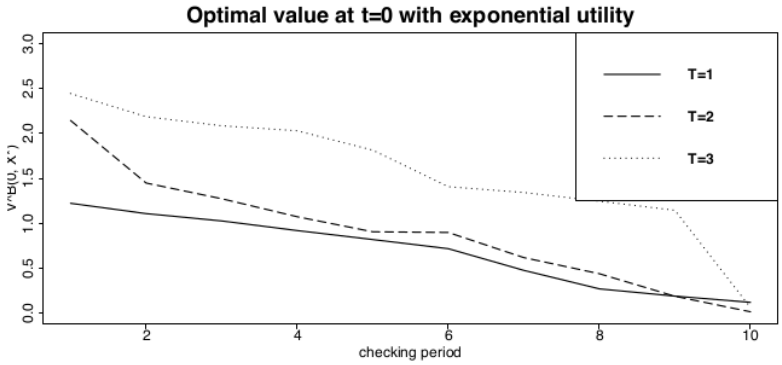

Figure 3.5: The simulated optimal result from 0.01 confidence level of the economy with jump process and piecewise exponential utility. The coefficient on the utility function is $\gamma_1 = \gamma_2 = 0.55$ and $\theta_1 = 1$, $\theta_2 = 2$.

Notice that in the $\alpha = 0.01$ confidence level, the results differ obviously between the piecewise power utility and the piecewise exponential utility, this might be due to the different bounds of the two functions as when $x \to \infty$, the piecewise power utility tends to infinity while the piecewise exponential utility tends to a finite value. We include a further examination of this phenomenon

in section 3.3.

3.2.2 The result with a geometric Brownian Motion

We now turn to the economy cases with geometric Brownian Motion. We first consider the risk constraint produced by Value at Risk and would expect the outcome from the Expected shortfall to be of a similar pattern, as the Expected Shortfall can be regarded as the conditional average of VaR.

From section 3.2.1, the risk constraint might be more efficient to the portfolio with a stock of higher total variation in the evaluation window, thus the simulation result of the expected maximal utility under this economy case is expected to be bounded more effectively with the same parameter.

For both confidence levels 0.05 and 0.01, we keep the coefficients of the piecewise power function and the piecewise exponential function as the same as those in the economy case with jump process, that is, we still let $\beta_1 = \beta_2 = 0.5$, $k = 2$, $\gamma_1 = \gamma_2 = 0.55$ and $\theta_1 = 1$, $\theta_2 = 2$ respectively.

Figure 3.6 shows the simulated result with the 0.05 confidence level and the piecewise power utility. As expected, the risk constraint is significantly more efficient in this economy case compared to the one with the jump process as it bounds the expected utility to a level that is much lower than what is shown in figure 3.4.

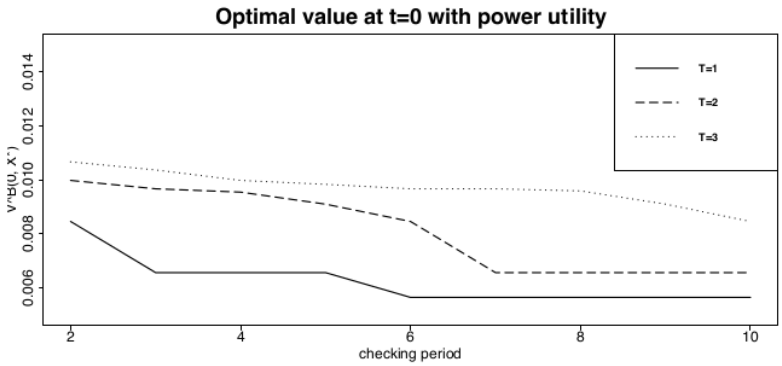

Figure 3.6: The simulated optimal result from 0.05 confidence level of the economy with geometric Brownian motion and piecewise power utility under the constraint deduced from VaR. The coefficient on the utility function is $\gamma_1 = \gamma_2 = 0.55$ and $\theta_1 = 1$, $\theta_2 = 2$.

Notice that we only show the result with 2 to 10 checking points in figure 3.6. This is due to an incredibly large number produced from trading horizon $T = 3$ when we had only one checking point. The result with one checking point is shown in table 3.2. The issue that causing this phenomenon is that the power utility function is unbounded with large profit and loss, and a larger trading horizon with a fixed number of checking points is more likely to have larger volatility.

Time Horizon	$T = 1$	$T = 2$	$T = 3$
1 checking point	9.0955×10^{-3}	3.0517	1.2144×10^{7}

Table 3.2: Simulated result under confidence level 0.05 using the piecewise power utility in the economy case with geometric Brownian Motion under 0.05 confidence level under the constraint deduced from VaR.

Figure 3.7 shows the result with 0.05 confidence level under piecewise exponential utility. Similar with section 3.2.1, the result from the piecewise exponential utility function is lower than the one from the piecewise power utility, which supports the discussion that the optimised expected utility is highly correlated to the shape of the utility function.

Figure 3.8 and 3.9 are results from the two utilities under $\alpha = 0.01$ confidence level without changing other parameters respectively. The decreasing trend in the increasing checking points

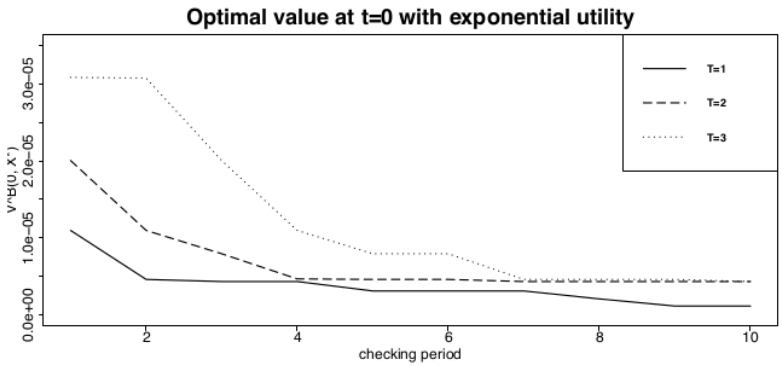

Figure 3.7: The simulated optimal result from 0.05 confidence level of the economy with geometric Brownian motion and piecewise exponential utility under the constraint deduced from VaR. The coefficient on the utility function is $\gamma_1 = \gamma_2 = 0.55$ and $\theta_1 = 1$, $\theta_2 = 2$.

still can be seen obviously. The result from the piecewise power utility is actually lower than those from $\alpha = 0.05$ confidence level with a fixed number of checking points, which is because the admissible set for Π^B is smaller than the one from the $\alpha = 0.05$ confidence level. Notice the result for terminal time $T = 3$ is less than that for time $T = 2$ from the piecewise power utility with more than 7 checking points, which might be due to the computational error from R as the resulting maximal value is rather small.

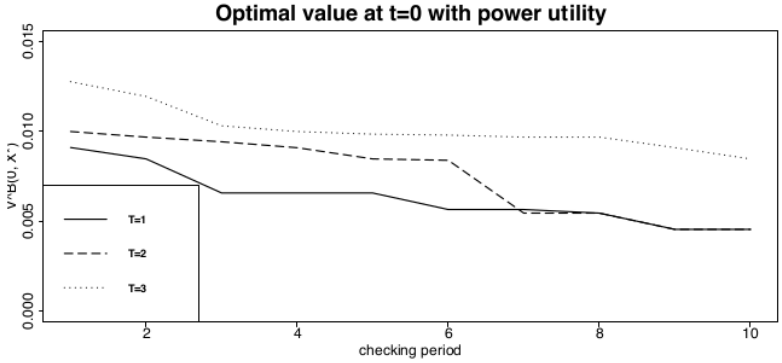

Figure 3.8: The simulated optimal result from 0.01 confidence level of the economy with geometric Brownian motion and piecewise power utility under the constraint deduced from VaR. The coefficient on the utility function is $\gamma_1 = \gamma_2 = 0.55$ and $\theta_1 = 1$, $\theta_2 = 2$.

We now consider performing the risk constraint produced by Expected Shortfall. Without changing any parameters, we would expect that the results will have a similar pattern as those from the Value at Risk measure.

Though the result from the piecewise power utility under confidence level $\alpha = 0.05$, shown as figure 3.10, has a larger value with 2 to 6 checking points compared with the one under the constraint deduced from VaR, the maximal expected value decreases faster to a similar level.

One interesting result is produced under the constraint by Expected Shortfall at $\alpha = 0.05$ confidence level. The maximal expected utility is the same as we have from the constraint by VaR at the current order of magnitude. Though expand the order will show the difference, we cannot tell if it is caused by different risk measures or just numerical error by this data set.

Figure 3.12 and figure 3.13 are results from $\alpha = 0.01$ confidence level of the piecewise power utility and piecewise exponential utility without changing other parameters respectively. Notice

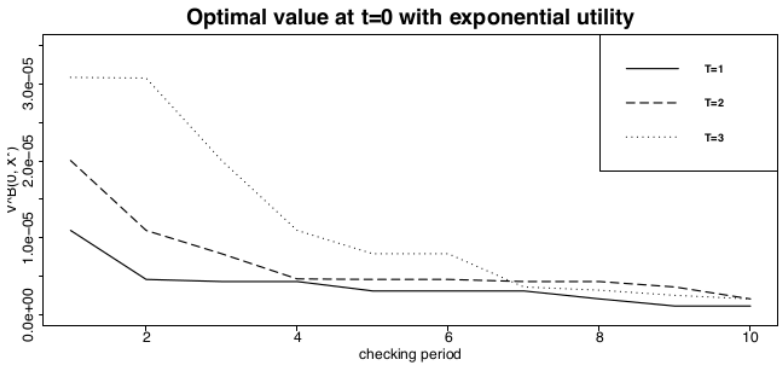

Figure 3.9: The simulated optimal result from 0.01 confidence level of the economy with geometric Brownian motion and piecewise exponential utility under the constraint deduced from VaR. The coefficient on the utility function is $\gamma_1 = \gamma_2 = 0.55$ and $\theta_1 = 1$, $\theta_2 = 2$.

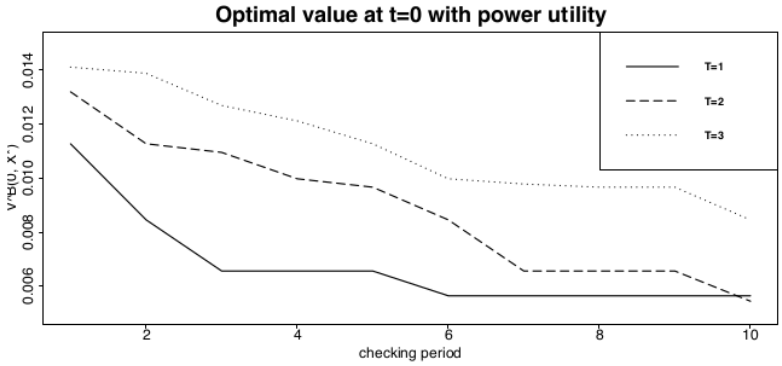

Figure 3.10: The simulated optimal result from 0.05 confidence level of the economy with geometric Brownian motion and piecewise power utility under the constraint deduced from ES. The coefficient on the utility function is $\gamma_1 = \gamma_2 = 0.55$ and $\theta_1 = 1$, $\theta_2 = 2$.

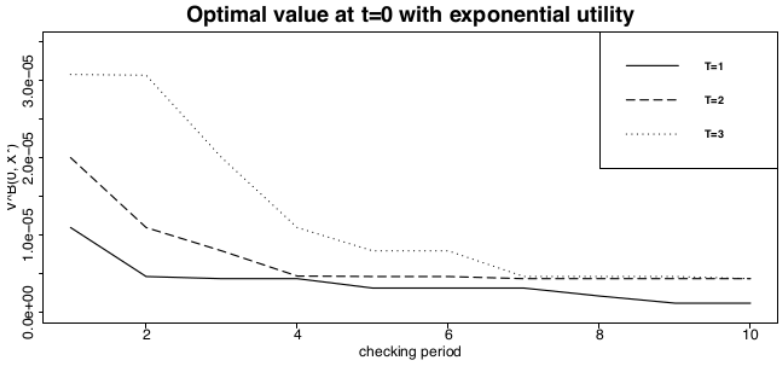

Figure 3.11: The simulated optimal result from 0.05 confidence level of the economy with geometric Brownian motion and piecewise exponential utility under the constraint deduced from ES. The coefficient on the utility function is $\gamma_1 = \gamma_2 = 0.55$ and $\theta_1 = 1$, $\theta_2 = 2$.

that compared with figure 3.8, the result shown in figure 3.12 deduced under the piecewise power utility is still larger than that from the Vale at Risk constraint with fewer checking points but with a faster rate of descent. There is still no difference between the two figures shown as 3.9 and 3.13 with the current order of magnitude.

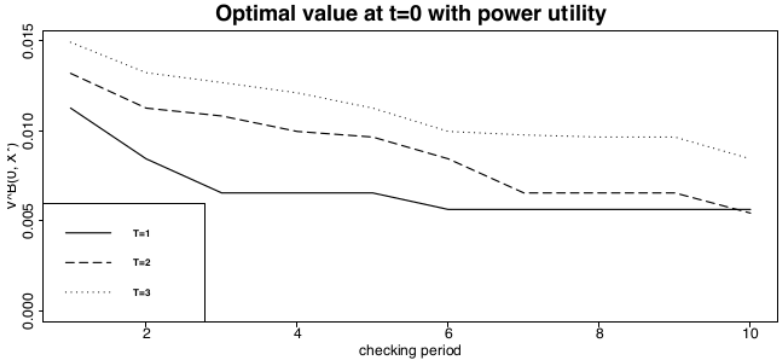

Figure 3.12: The simulated optimal result from 0.01 confidence level of the economy with geometric Brownian motion and piecewise power utility under the constraint deduced from ES. The coefficient on the utility function is $\gamma_1 = \gamma_2 = 0.55$ and $\theta_1 = 1$, $\theta_2 = 2$.

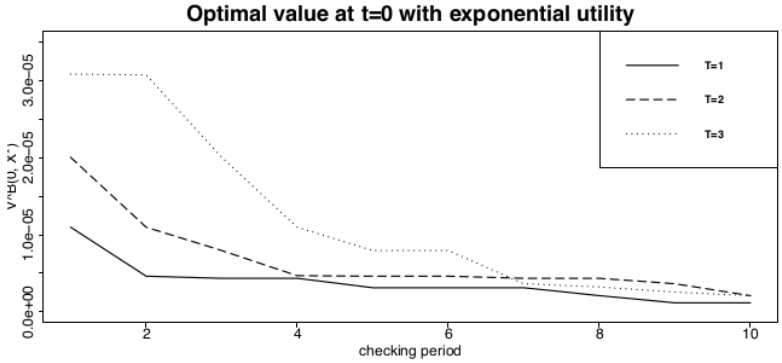

Figure 3.13: The simulated optimal result from 0.01 confidence level of the economy with geometric Brownian motion and piecewise exponential utility under the constraint deduced from ES. The coefficient on the utility function is $\gamma_1 = \gamma_2 = 0.55$ and $\theta_1 = 1$, $\theta_2 = 2$.

3.3 Impact of utility functions

To further examine the impact of the shape of the utility function, we consider another S-shaped utility given as

$$U(x) = \begin{cases} x^\gamma/\gamma, & x \geq 0 \\ -|x|^\gamma/\gamma, & x < 0 \end{cases} \tag{3.3.1}$$

which just extends the CRRA utility to the negative profit domain shown in figure 3.14.

We would expect that the result will decrease as the value of γ increases with the coefficient value shown in figure 3.14 but without changing other parameters of the two economy cases.

Table 3.3 shows the result with confidence level $\alpha = 0.01$ under the economy cases with the jump process with terminal horizon $T = 1$, which, as we expect, the outcome shrinks with the decreasing γ.

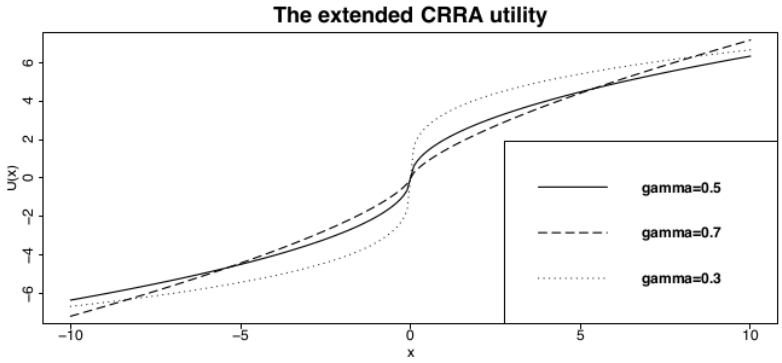

Figure 3.14: The extended CRRA utility.

Coefficient value	$\gamma = 0.7$	$\gamma = 0.5$	$\gamma = 0.3$
1 checking point	6.9458×10^{18}	1.2029×10^{11}	6.7771×10^{3}
2 checking points	2.0827×10^{16}	2.9271×10^{8}	5.7672×10^{3}
3 checking points	5.5463×10^{11}	3.9431×10^{5}	5.4314×10^{2}
4 checking points	8.0515×10^{8}	1.6293×10^{5}	3.9563×10
5 checking points	3.1379×10^{8}	7.1926×10^{4}	3.9001×10
6 checking points	7.9062×10^{7}	2.4520×10^{4}	2.4560×10
7 checking points	5.4318×10^{7}	3.3672×10^{2}	2.3225×10
8 checking points	2.2243×10^{4}	9.1391×10	1.9891×10
9 checking points	8.0124×10^{2}	8.7934×10	1.2665×10
10 checking points	7.1770×10^{2}	6.9029×10	1.70160

Table 3.3: Simulated result under confidence level 0.01 using the extended CRRA utility in the economy case with jump process with trading horizon $T = 1$.

To further analyse the impact of the shape of the utility under the positive-loss domain, we manipulate the extended CRRA model slightly into

$$U(x) = \begin{cases} x_1^{\gamma}/\gamma_1, & x \geq 0 \\ -|x|_2^{\gamma}/\gamma_2, & x < 0 \end{cases}$$

with fixed $\gamma_1 = 0.5$ and $\gamma_2 \in \{0.3, 0.7, 0.9\}$ which is shown as figure 3.15. Table B.14 shows

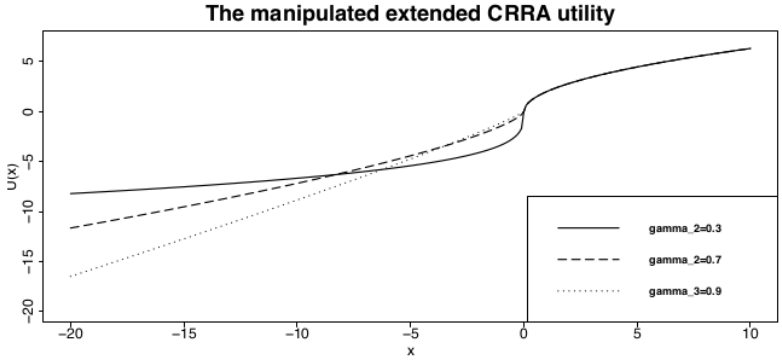

Figure 3.15: The manipulated extended CRRA utility.

the result from conscience level $\alpha = 0.05$ under the economy cases with the geometric Brownian Motion and risk constraint produced by VaR without changing other model parameters. Notice that besides the decreasing trend of the maximal expected utility over the number of checking points, the resulting value is also positively related to γ_2, which controls the slope of the utility function in the positive loss domain.

Coefficient value	$\gamma_2 = 0.9$	$\gamma_2 = 0.7$	$\gamma_2 = 0.3$
1 checking point	2.9687×10^{-2}	1.5861×10^{-3}	1.9384×10^{-4}
2 checking points	27794×10^{-2}	1.2791×10^{-3}	1.8805×10^{-4}
3 checking points	2.6465×10^{-2}	1.1026×10^{-3}	1.8805×10^{-4}
4 checking points	2.4292×10^{-2}	1.1026×10^{-3}	1.6590×10^{-4}
5 checking points	2.4292×10^{-2}	1.0104×10^{-3}	1.6590×10^{-4}
6 checking points	2.1584×10^{-2}	1.0103×10^{-3}	1.6590×10^{-4}
7 checking points	21583×10^{-2}	1.0103×10^{-3}	1.4214×10^{-4}
8 checking points	2.1583×10^{-2}	5.0570×10^{-4}	1.4214×10^{-4}
9 checking points	1.8035×10^{-2}	5.0569×10^{-4}	1.1644×10^{-4}
10 checking points	1.8035×10^{-2}	3.6351×10^{-4}	5.6780×10^{-5}

Table 3.4: Simulated result under confidence level 0.05 using the extended CRRA utility in the economy case with geometric Brownian Motion with trading horizon $T = 1$.

A similar result is produced if we instead fix γ_2 to be 0.5 and let $\gamma_1 \in \{0.3, 0.7, 0.9\}$, which indicates that the resulting optimised expected utility certainly heavily depends not only on the portfolio price but also on the shape of the utility function.

If an ES constraint is imposed instead, the resulting pattern is similar to what we have from the VaR constraint, thus we do not include the numerical result in this section.

From the results in this subsection and in the previous two sections, we can conclude that the efficiency of the risk constraint heavily depends on the shape of the utility function. Suppose the range of the utility is bounded. In that case, the maximal expected utility is of cause not possible to tend to infinity, while with a utility function that is unlimited, the result will be then highly related to the slope of the function at extremal value with a fixed number of checking points, which is not out of surprise as with a utility that grows slowly to infinity the outcome with extremal losses and gains should not be greater than the one of the same range but with rapid growth.

3.4 Summary of discussions

As shown in section 3.2, the maximal expected utility decreases in trend with the increasing number of checking points in the sense that the resulting value is heavily related to the shape and range of the corresponding utility function. If the utility function $U(x)$ is unbounded and goes to infinity with $x \to \infty$, the resulting V_0 is more likely to tend to a large value with a small number of checking points. Overall adding enough checking points can limit the optimised expected utility to an acceptable value.

Each checking point imposed on the trading process has its efficiency in the sense that it seems to be more effective to stock with higher total variation in the corresponding evaluation window if the variance of the stock is greater than zero.

As the terminal horizon T increases, the resulting maximal utility under given constraints with fixed checking points is expected to increase as well.

Due to the different projecting distributions in the two economy cases, increasing the confidence level α will result in a larger admissible set for the economy with jump process but a smaller one with geometric Brownian Motion, which leads to different trends of the maximal expected utility over the confidence level.

Using a dynamic risk constraint deduced from Expected Shortfall will generally result in a higher maximal expected utility than from Value at Risk with a small number of checking points, except for having only one checking time with the piecewise power utility. This exceptional might be due to the unbounded range of the piecewise power utility function, which also leads to the ineffectiveness when imposing a dynamic risk constraint with $\alpha = 0.01$ confidence level.

Conclusion

Value at Risk and Expected Shortfall are widely used in the industry while the impact of imposing them as trading risk constraints has not been studied extensively. Armstrong & Brigo (2019*b*) show that when using a static risk constraint deduced from these two risk measures, the maximal expected utility of a tail-risk-seeking trader will be unlimited. Results from Armstrong et al. (2020) indicate that if the risk constraint is dynamic instead, meaning that one imposes the constraint through the whole trading process, the maximal expected utility of the trader can be bounded effectively. This paper fills the gap between these two findings. We proved that if the dynamic risk constraint is imposed only in a finite number of checking times, the resulting maximal expected utility can still be bounded in the sense that the resulting value is decreasing when the number of checking points increases. Though the resulting value is highly related to the range and shape of the corresponding utility function, adding enough checking points can bound the maximal expected utility to an acceptable level.

We achieve this by extending the original LSMC method to endogenous heteroskedastic states with S-shaped utility and applying a transformation to the concave utility to reduce the simulation bias caused by the non-linearity of the utility function. This extended method can be applied to general optimisation problems with S-shaped utility if a differentiable and invertible transformation function exits.

However, the analysis in this paper does not include the assumption that traders have access to derivative markets, which might still make the dynamic risk constraint inefficient if only a finite number of checking points are imposed. Another possible research direction is that the extended LSMC algorithm we introduced is indeed computationally heavy, and there might exist some techniques to simplify the method and improve the speed.

Appendix A

Technical Proofs

A.1 Proof sketch of proposition 1.3.2

We provide the sketch of proof for proposition 1.3.2 from Armstrong et al. (2020) as follows.

Without losing of generality, we only need to consider time $t = 0$. By Karatzas et al. (1987), the optimisation problem (1.3.1) with $K = K_0$ is equivalent to the problem of the form

$$\begin{cases} V(0, x_0) = \sup_{X_T \in \mathcal{F}_T} \mathbb{E}[U(X_T)] \\ \mathbb{E}[\xi_T X_T] \leq x_0, \end{cases}$$

where

$$\xi_T := \exp\left[\left(-\frac{\mu - r}{\sigma}\right) W_T - \left(r + \frac{1}{2}\left(\frac{\mu - r}{\sigma}\right)^2\right) T\right]$$

is the pricing kernel of the economy with geometric Brownian Motion, the one with the jump process needs to be re-calculated. Now we consider a digital option with a payoff

$$X_T = -\frac{b}{\mathbb{P}(\xi_T > k)} \mathbb{1}_{(\xi_T > k)} + b \mathbb{1}_{(\xi_T \leq k)}$$

with $b > 0$ and $k > 0$. The constraint on the budget is then

$$-\frac{b}{\mathbb{P}(\xi_T > k)} \mathbb{E}\left[\xi_T \mathbb{1}_{(\xi_T > k)}\right] + b\mathbb{E}\left[\xi_T \mathbb{1}_{(\xi_T \leq k)}\right] \leq x_0,$$

which leads to

$$-b \leq \frac{\mathbb{P}(\xi_T > k)}{\mathbb{E}\left[\xi_T \mathbb{1}_{(\xi_T > k)}\right]} \left[x_0 - b\mathbb{E}\left[\xi_T \mathbb{1}_{(\xi_T \leq k)}\right]\right]$$

Since ξ_T is bounded from above, we have

$$\lim_{k \to \infty} \frac{\mathbb{P}(\xi_T > k)}{\mathbb{E}\left[\xi_T^1 (\xi_T > k)\right]} = 0.$$

For any fixed $b > 0$, we can find a large enough k to satisfy the budget constraint.

Hence, the value function should not be less than the expected utility as

$$V_0(0, x_0) \geq U\left(-\frac{b}{\mathbb{P}(\xi_T > k)}\right) \mathbb{P}(\xi_T > k) + U(b) \mathbb{P}(\xi_T < k).$$

By assumption 1.3.1, $\lim_{x \to -\infty} \frac{U(x)}{x} = 0$. Thus, by letting $k \to \infty$w, we have $V_0(0, x_0) \geq U(b)$. Since b is taken arbitrarily, the result then follows.

A.2 Solution of equation (2.6.2)

We provide the solution to the numerical example in section 2.6.

We first consider a simplified optimisation problem without the allocation δ_t, since we are considering the general problem in the form of equation (2.6.1), the optimisation problem can be re-written as

$$V_0(x) = \sup_{\Pi} \mathbb{E}\left[\sum_{i=0}^{n-1} \frac{(\alpha_{t_i} X_{t_i})^\gamma}{\gamma} \mid X_{t_0} = x; \Pi\right].$$

Let the stochastic component in the transition function be ξ_{t_i}, then we can follow the process by Samuelson (1975) to solve the problem.

At the terminal time $t_n = T$, the value function is of the form

$$V_{t_n}(X_{t_n}) = \frac{(\alpha_{t_n} X_{t_n})^\gamma}{\gamma}$$

Notice that since no utility will be gained from the saving account, the optimal decision is to consume all the money, leading to $\alpha_{t_n} = 1$.

At time $t = t_{n-1}$, the value function can then be written as

$$\begin{aligned} V_{t_{n-1}}(X_{t_{n-1}}) &= \frac{(\alpha_{t_{n-1}} X_{t_{n-1}})^\gamma}{\gamma} + \mathbb{E}\left[V_{t_n}(X_{t_n})\right] \\ &= \frac{(\alpha_{t_{n-1}} X_{t_{n-1}})^\gamma}{\gamma} + \frac{\left((1-\alpha_{t_{n-1}}) X_{t_{n-1}}\right)^\gamma \mathbb{E}\left[\xi_{t_{n-1}}^\gamma\right]}{\gamma}. \end{aligned}$$

o find the optimal $\alpha_{t_{n-1}}$, we differentiate the value function with respect to $\alpha_{t_{n-1}}$ and equating the differentiation to zero, hence we have

$$\frac{\partial V_{t_{n-1}}}{\partial \alpha_{t_{n-1}}} = X_{t_{n-1}} (\alpha_{t_{n-1}} X_{t_{n-1}})^{\gamma-1} - X_{t_{n-1}} \left((1-\alpha_{t_{n-1}}) X_{t_{n-1}}\right)^{\gamma-1} \mathbb{E}\left[\xi_{t_{n-1}}^\gamma\right] = 0,$$

thus we have

$$\alpha_{t_{n-1}} = (1-\alpha_{t_{n-1}}) \mathbb{E}\left[\xi_{t_{n-1}}^\gamma\right]^{\frac{1}{\gamma-1}}$$

which can be re-written as

$$\alpha_{t_{n-1}} = \left(1 + \mathbb{E}\left[\xi_{t_{n-1}}^\gamma\right]^{\frac{1}{1-\gamma}}\right)^{-1}.$$

Now, if the price of the portfolio depends on the risk allocation variable δ_t, for our model that is, $\xi_{t_{n-1}} = e^{\delta_{t_{n-1}} Z_{t_{n-1}} + (1-\delta_{t_{n-1}}) r_{t_{n-1}}}$, then we can follow the similar step as above to find the optimal risky asset allocation. Since we assume $Z_t \overset{i.i.d}{\sim} \mathcal{N}(\mu, \sigma^2)$, we then have

$$\frac{\partial V_{t_{n-1}}}{\partial \delta_{t_{n-1}}} = \mathbb{E}\left[(Z_{t_n} - r)\left((1-\alpha_{t_{n-1}}) X_{t_{n-1}}\right)^\gamma \xi_{t_{n-1}}^\gamma\right],$$

equating it to zero, we then have

$$\delta_{t_{n-1}} = \frac{r-\mu}{\gamma\sigma^2}.$$

Hence the maximal value of the function $V_{t_{n-1}}$ is

$$\begin{aligned} V_{t_{n-1}}(X_{t_{n-1}}) &= \frac{(\alpha_{t_{n-1}} X_{t_{n-1}})^\gamma}{\gamma} + \frac{\left((1-\alpha_{t_{n-1}}) X_{t_{n-1}}\right)^\gamma \mathbb{E}\left[\xi_{t_{n-1}}^\gamma\right]}{\gamma} \\ &= \frac{(X_{t_{n-1}})^\gamma}{\gamma}\left((\alpha_{t_{n-1}})^\gamma + (1-\alpha_{t_{n-1}})^\gamma\right) \mathbb{E}\left[\xi_{t_{n-1}}^\gamma\right] \\ &= \frac{(X_{t_{n-1}})^\gamma}{\gamma}(\alpha_{t_{n-1}})^{\gamma-1}. \end{aligned}$$

We then use this value into the next iteration. By repeating this process until $t = 0$, we finally have

$$\alpha_{t_i} = \begin{cases} 1, & \text{if } i = n \\ \left(1 + \left(\mathbb{E}\left[\xi_{t_i}^\gamma\right] \alpha_{t_{i+1}}^{\gamma-1}\right)^{\frac{1}{1-\gamma}}\right)^{-1}, & \text{otherwise.} \end{cases},$$

and hence

$$\alpha_{t_i} = \begin{cases} 1, & \text{if } i = n \\ \left(1 + \left(e^{\gamma\delta_{t_i}\mu + \gamma^2\delta_{t_i}^2\sigma^2/2 + \left(1-\delta_{t_i}\right)\gamma r}\alpha_{t_{i+1}}^{\gamma-1}\right)^{\frac{1}{1-\gamma}}\right)^{-1}. & \text{otherwise} \end{cases}$$

Appendix B

Results of the simulation

B.1 Results of the economy with jump process

Time Horizon	$T = 1$	$T = 2$	$T = 3$
1 checking point	8.4677×10^{-1}	1.6718	2.3754
2 checking points	8.2686×10^{-1}	1.4392	1.7922
3 checking points	7.5629×10^{-1}	1.2928	1.4972
4 checking points	5.0886×10^{-1}	1.1367	1.3155
5 checking points	4.6979×10^{-1}	7.0387×10^{-1}	1.2941
6 checking points	3.7223×10^{-1}	5.5411×10^{-1}	7.5022×10^{-1}
7 checking points	3.1376×10^{-1}	5.0002×10^{-1}	6.2967×10^{-1}
8 checking points	2.3499×10^{-1}	3.6227×10^{-1}	4.0677×10^{-1}
9 checking points	1.8301×10^{-1}	2.3405×10^{-1}	3.2409×10^{-1}
10 checking points	3.0079×10^{-2}	7.5631×10^{-2}	3.1946×10^{-1}

Table B.1: Simulated result under confidence level 0.05 using piecewise power utility function in the economy case with jump process. The coefficient on the utility function is $\beta_1 = \beta_2 = 0.5$ and $k = 2$.

Time Horizon	$T = 1$	$T = 2$	$T = 3$
1 checking point	1.1839	1.5264	3.2686
2 checking points	9.9229×10^{-1}	1.4390	2.4767
3 checking points	7.2219×10^{-1}	1.3499	2.0094
4 checking points	6.1169×10^{-1}	1.2273	1.9403
5 checking points	5.5286×10^{-1}	8.5368×10^{-1}	1.8352
6 checking points	5.2642×10^{-1}	7.3117×10^{-1}	1.0845
7 checking points	5.2170×10^{-1}	6.5741×10^{-1}	1.0540
8 checking points	4.9382×10^{-1}	5.5188×10^{-1}	1.0249
9 checking points	3.5524×10^{-1}	5.4326×10^{-1}	6.6103×10^{-1}
10 checking points	5.8072×10^{-2}	9.8917×10^{-2}	5.6126×10^{-2}

Table B.2: Simulated result under confidence level 0.05 using piecewise exponential utility function in the economy case with jump process. The coefficient on the utility function is $\gamma_1 = \gamma_2 = 0.55$ and $\theta_1 = 1$, $\theta_2 = 2$.

Time Horizon	$T=1$	$T=2$	$T=3$
1 checking point	7.9723×10^{9}	1.6829×10^{13}	3.5817×10^{18}
2 checking points	4.9276×10^{9}	2.8615×10^{10}	9.0724×10^{10}
3 checking points	5.1721×10^{8}	1.7918×10^{9}	8.2459×10^{10}
4 checking points	7.6527×10^{7}	3.1457×10^{8}	2.0380×10^{9}
5 checking points	2.8970×10^{7}	1.5445×10^{8}	8.0277×10^{8}
6 checking points	5.7796×10^{6}	1.7270×10^{7}	1.7368×10^{8}
7 checking points	2.2745×10^{6}	4.8567×10^{6}	3.6777×10^{6}
8 checking points	1.4715×10^{5}	2.7427×10^{5}	2.7886×10^{6}
9 checking points	1.5282×10^{2}	6.1647×10^{4}	1.2227×10^{5}
10 checking points	8.5393×10	1.2140×10^{2}	1.7256×10^{4}

Table B.3: Simulated result under confidence level 0.01 using piecewise power utility function in the economy case with jump process. The coefficient on the utility function is $\beta_1 = \beta_2 = 0.5$ and $k = 2$.

Time Horizon	$T=1$	$T=2$	$T=3$
1 checking point	1.2223	2.1420	2.4421
2 checking points	1.1077	1.4475	2.1849
3 checking points	1.0264	1.2733	2.0837
4 checking points	9.1929×10^{-1}	1.0732	2.0281
5 checking points	8.1960×10^{-1}	9.0591×10^{-1}	1.8128
6 checking points	7.1809×10^{-1}	8.9837×10^{-1}	1.4069
7 checking points	4.7712×10^{-1}	6.1916×10^{-1}	1.3425
8 checking points	2.7159×10^{-1}	4.4000×10^{-1}	1.2460
9 checking points	1.9095×10^{-1}	1.8961×10^{-1}	1.1449
10 checking points	1.2182×10^{-2}	1.7062×10^{-2}	6.5387×10^{-2}

Table B.4: Simulated result under confidence level 0.01 using piecewise exponential utility function in the economy case with jump process. The coefficient on the utility function is $\gamma_1 = \gamma_2 = 0.55$ and $\theta_1 = 1$, $\theta_2 = 2$.

B.2 Results of the economy with geometric Brownian Motion

Time Horizon	$T=1$	$T=2$	$T=3$
1 checking point	9.0955×10^{-3}	3.0517	1.2144×10^{8}
2 checking points	8.4569×10^{-3}	9.9776×10^{-3}	1.0665×10^{-2}
3 checking points	6.5627×10^{-3}	9.6674×10^{-3}	1.0365×10^{-2}
4 checking points	6.5627×10^{-3}	9.5442×10^{-3}	9.9776×10^{-3}
5 checking points	6.5627×10^{-3}	9.0980×10^{-3}	9.8326×10^{-3}
6 checking points	5.6450×10^{-3}	8.4569×10^{-3}	9.6674×10^{-3}
7 checking points	5.6450×10^{-3}	6.5627×10^{-3}	9.6674×10^{-3}
8 checking points	5.6450×10^{-3}	6.5627×10^{-3}	9.5894×10^{-3}
9 checking points	5.6450×10^{-3}	6.5627×10^{-3}	9.1003×10^{-3}
10 checking points	5.6450×10^{-3}	6.5627×10^{-3}	8.4570×10^{-3}

Table B.5: Simulated optimal result from 0.05 confidence level of the economy with geometric Brownian motion and piecewise power utility under the constraint deduced from VaR. The coefficient on the utility function is $\gamma_1 = \gamma_2 = 0.55$ and $\theta_1 = 1$, $\theta_2 = 2$.

Time Horizon	$T=1$	$T=2$	$T=3$
1 checking point	1.0981×10^{-5}	2.0042×10^{-5}	3.0821×10^{-5}
2 checking points	4.6315×10^{-6}	1.0981×10^{53}	3.0729×10^{-5}
3 checking points	4.3559×10^{-6}	7.9597×10^{-6}	2.0042×10^{-5}
4 checking points	4.3559×10^{-6}	4.6955×10^{-6}	1.0981×10^{-5}
5 checking points	3.1352×10^{-6}	4.6955×10^{-6}	7.9597×10^{-6}
6 checking points	3.1352×10^{-6}	4.6955×10^{-6}	7.9597×10^{-6}
7 checking points	3.1352×10^{-6}	4.3559×10^{-6}	4.6315×10^{-6}
8 checking points	2.1055×10^{-6}	4.3559×10^{-6}	4.6315×10^{-6}
9 checking points	1.1795×10^{-6}	4.3559×10^{-6}	4.6315×10^{-6}
10 checking points	1.1795×10^{-6}	4.3559×10^{-6}	4.3559×10^{-6}

Table B.6: Simulated optimal result from 0.05 confidence level of the economy with geometric Brownian motion and piecewise exponential utility under the constraint deduced from VaR. The coefficient on the utility function is $\gamma_1 = \gamma_2 = 0.55$ and $\theta_1 = 1$, $\theta_2 = 2$.

Time Horizon	$T=1$	$T=2$	$T=3$
1 checking point	9.0890×10^{-3}	9.9776×10^{-3}	1.2746×10^{-2}
2 checking points	8.4569×10^{-3}	9.6674×10^{-3}	1.1927×10^{-2}
3 checking points	6.5627×10^{-3}	9.4093×10^{-3}	1.0295×10^{-2}
4 checking points	6.5627×10^{-3}	9.0788×10^{-3}	9.9776×10^{-3}
5 checking points	6.5627×10^{-3}	8.4569×10^{-3}	9.8326×10^{-3}
6 checking points	5.6450×10^{-3}	8.3802×10^{-3}	9.7803×10^{-3}
7 checking points	5.6450×10^{-3}	5.4444×10^{-3}	9.6675×10^{-3}
8 checking points	5.4444×10^{-3}	5.4444×10^{-3}	9.6675×10^{-3}
9 checking points	4.5414×10^{-3}	4.5414×10^{-3}	9.0845×10^{-3}
10 checking points	4.5414×10^{-3}	4.5414×10^{-3}	8.4569×10^{-3}

Table B.7: Simulated optimal result from 0.01 confidence level of the economy with geometric Brownian motion and piecewise power utility under the constraint deduced from VaR. The coefficient on the utility function is $\gamma_1 = \gamma_2 = 0.55$ and $\theta_1 = 1$, $\theta_2 = 2$.

Time Horizon	$T=1$	$T=2$	$T=3$
1 checking point	1.0981×10^{-5}	2.0042×10^{-5}	3.0821×10^{-5}
2 checking points	4.6315×10^{-6}	1.0981×10^{53}	3.0729×10^{-5}
3 checking points	4.3559×10^{-6}	7.9597×10^{-6}	2.0042×10^{-5}
4 checking points	4.3559×10^{-6}	4.6955×10^{-6}	1.0981×10^{-5}
5 checking points	3.1352×10^{-6}	4.6315×10^{-6}	7.9597×10^{-6}
6 checking points	3.1352×10^{-6}	4.6315×10^{-6}	7.9597×10^{-6}
7 checking points	3.1352×10^{-6}	4.3559×10^{-6}	3.6513×10^{-6}
8 checking points	2.1055×10^{-6}	4.3559×10^{-6}	3.6513×10^{-6}
9 checking points	1.1795×10^{-6}	3.6513×10^{-6}	2.5675×10^{-6}
10 checking points	1.1795×10^{-6}	2.1055×10^{-6}	2.1055×10^{-6}

Table B.8: Simulated optimal result from 0.01 confidence level of the economy with geometric Brownian motion and piecewise exponential utility under the constraint deduced from VaR. The coefficient on the utility function is $\gamma_1 = \gamma_2 = 0.55$ and $\theta_1 = 1$, $\theta_2 = 2$.

Time Horizon	$T=1$	$T=2$	$T=3$
1 checking point	1.1270×10^{-2}	1.3196×10^{-2}	1.4113×10^{-2}
2 checking points	8.4569×10^{-3}	1.1275×10^{-2}	1.3885×10^{-2}
3 checking points	6.5627×10^{-3}	1.0955×10^{-2}	1.2693×10^{-2}
4 checking points	6.5627×10^{-3}	9.9786×10^{-3}	1.2122×10^{-2}
5 checking points	6.5627×10^{-3}	9.6674×10^{-3}	1.1274×10^{-2}
6 checking points	5.6450×10^{-3}	8.4570×10^{-3}	9.9786×10^{-3}
7 checking points	5.6450×10^{-3}	6.5627×10^{-3}	9.7847×10^{-3}
8 checking points	5.6450×10^{-3}	6.5627×10^{-3}	9.6674×10^{-3}
9 checking points	5.6450×10^{-3}	6.5627×10^{-3}	9.6674×10^{-3}
10 checking points	5.6450×10^{-3}	5.4444×10^{-3}	8.4570×10^{-3}

Table B.9: Simulated optimal result from 0.05 confidence level of the economy with geometric Brownian motion and piecewise power utility under the constraint deduced from ES. The coefficient on the utility function is $\gamma_1 = \gamma_2 = 0.55$ and $\theta_1 = 1$, $\theta_2 = 2$.

Time Horizon	$T=1$	$T=2$	$T=3$
1 checking point	1.0981×10^{-5}	2.0042×10^{-5}	3.0821×10^{-5}
2 checking points	4.6315×10^{-6}	1.0981×10^{53}	3.0729×10^{-5}
3 checking points	4.3559×10^{-6}	7.9597×10^{-6}	2.0042×10^{-5}
4 checking points	4.3559×10^{-6}	4.6955×10^{-6}	1.0981×10^{-5}
5 checking points	3.1352×10^{-6}	4.6955×10^{-6}	7.9597×10^{-6}
6 checking points	3.1352×10^{-6}	4.6955×10^{-6}	7.9597×10^{-6}
7 checking points	3.1352×10^{-6}	4.3559×10^{-6}	4.6315×10^{-6}
8 checking points	2.1055×10^{-6}	4.3559×10^{-6}	4.6315×10^{-6}
9 checking points	1.1795×10^{-6}	4.3559×10^{-6}	4.6315×10^{-6}
10 checking points	1.1795×10^{-6}	4.3559×10^{-6}	4.3559×10^{-6}

Table B.10: Simulated optimal result from 0.05 confidence level of the economy with geometric Brownian motion and piecewise exponential utility under the constraint deduced from ES. The coefficient on the utility function is $\gamma_1 = \gamma_2 = 0.55$ and $\theta_1 = 1$, $\theta_2 = 2$.

Time Horizon	$T=1$	$T=2$	$T=3$
1 checking point	1.1275×10^{-2}	1.3205×10^{-2}	1.4932×10^{-2}
2 checking points	8.4570×10^{-3}	1.1275×10^{-2}	1.3243×10^{-2}
3 checking points	6.5627×10^{-3}	1.0839×10^{-2}	1.2698×10^{-2}
4 checking points	6.5627×10^{-3}	9.9786×10^{-3}	1.2122×10^{-2}
5 checking points	6.5627×10^{-3}	9.6674×10^{-3}	1.1274×10^{-2}
6 checking points	5.6450×10^{-3}	8.4570×10^{-3}	9.9786×10^{-3}
7 checking points	5.6450×10^{-3}	6.5628×10^{-3}	9.7847×10^{-3}
8 checking points	5.6450×10^{-3}	6.5628×10^{-3}	9.6675×10^{-3}
9 checking points	5.6450×10^{-3}	6.5628×10^{-3}	9.6675×10^{-3}
10 checking points	5.6450×10^{-3}	5.4444×10^{-3}	8.4569×10^{-3}

Table B.11: Simulated optimal result from 0.01 confidence level of the economy with geometric Brownian motion and piecewise power utility under the constraint deduced from ES. The coefficient on the utility function is $\gamma_1 = \gamma_2 = 0.55$ and $\theta_1 = 1$, $\theta_2 = 2$.

Time Horizon	$T=1$	$T=2$	$T=3$
1 checking point	1.0981×10^{-5}	2.0042×10^{-5}	3.0821×10^{-5}
2 checking points	4.6315×10^{-6}	1.0981×10^{53}	3.0729×10^{-5}
3 checking points	4.3559×10^{-6}	7.9597×10^{-6}	2.0042×10^{-5}
4 checking points	4.3559×10^{-6}	4.6955×10^{-6}	1.0981×10^{-5}
5 checking points	3.1352×10^{-6}	4.6315×10^{-6}	7.9597×10^{-6}
6 checking points	3.1352×10^{-6}	4.6315×10^{-6}	7.9597×10^{-6}
7 checking points	3.1352×10^{-6}	4.3559×10^{-6}	3.6513×10^{-6}
8 checking points	2.1055×10^{-6}	4.3559×10^{-6}	3.6513×10^{-6}
9 checking points	1.1795×10^{-6}	3.6513×10^{-6}	2.5675×10^{-6}
10 checking points	1.1795×10^{-6}	2.1055×10^{-6}	2.1055×10^{-6}

Table B.12: Simulated optimal result from 0.01 confidence level of the economy with geometric Brownian motion and piecewise exponential utility under the constraint deduced from ES. The coefficient on the utility function is $\gamma_1 = \gamma_2 = 0.55$ and $\theta_1 = 1$, $\theta_2 = 2$.

B.3 Results from the extended CRRA utility

Coefficient value	$\gamma_2 = 0.9$	$\gamma_2 = 0.7$	$\gamma_2 = 0.3$
1 checking point	2.9687×10^{-2}	1.5861×10^{-3}	1.9384×10^{-4}
2 checking points	27794×10^{-2}	1.2791×10^{-3}	1.8805×10^{-4}
3 checking points	2.6465×10^{-2}	1.1026×10^{-3}	1.8805×10^{-4}
4 checking points	2.4292×10^{-2}	1.1026×10^{-3}	1.6590×10^{-4}
5 checking points	2.4292×10^{-2}	1.0104×10^{-3}	1.6590×10^{-4}
6 checking points	2.1584×10^{-2}	1.0103×10^{-3}	1.6590×10^{-4}
7 checking points	21583×10^{-2}	1.0103×10^{-3}	1.4214×10^{-4}
8 checking points	2.1583×10^{-2}	5.0570×10^{-4}	1.4214×10^{-4}
9 checking points	1.8035×10^{-2}	5.0569×10^{-4}	1.1644×10^{-4}
10 checking points	1.8035×10^{-2}	3.6351×10^{-4}	5.6780×10^{-5}

Table B.13: Simulated result under confidence level 0.05 using the extended CRRA utility in the economy case with geometric Brownian Motion with trading horizon $T = 1$.

Coefficient value	$\gamma_2 = 0.9$	$\gamma_2 = 0.7$	$\gamma_2 = 0.3$
1 checking point	2.9687×10^{-2}	1.5861×10^{-3}	1.9384×10^{-4}
2 checking points	27794×10^{-2}	1.2791×10^{-3}	1.8805×10^{-4}
3 checking points	2.6465×10^{-2}	1.1026×10^{-3}	1.8805×10^{-4}
4 checking points	2.4292×10^{-2}	1.1026×10^{-3}	1.6590×10^{-4}
5 checking points	2.4292×10^{-2}	1.0104×10^{-3}	1.6590×10^{-4}
6 checking points	2.1584×10^{-2}	1.0103×10^{-3}	1.6590×10^{-4}
7 checking points	21583×10^{-2}	1.0103×10^{-3}	1.4214×10^{-4}
8 checking points	2.1583×10^{-2}	5.0570×10^{-4}	1.4214×10^{-4}
9 checking points	1.8035×10^{-2}	5.0569×10^{-4}	1.1644×10^{-4}
10 checking points	1.8035×10^{-2}	3.6351×10^{-4}	5.6780×10^{-5}

Table B.14: Simulated result under confidence level 0.05 using the extended CRRA utility in the economy case with geometric Brownian Motion with trading horizon $T = 1$.

Bibliography

Andreasson, J. & Shevchenko, P. V. (2019), 'Bias-corrected least-squares monte carlo for utility based optimal stochastic control problems', *Available at SSRN 2985828* .

Armstrong, J. & Brigo, D. (2018), 'Rogue traders versus value-at-risk and expected shortfall'.

Armstrong, J. & Brigo, D. (2019*a*), 'The ineffectiveness of coherent risk measures', *arXiv preprint arXiv:1902.10015* .

Armstrong, J. & Brigo, D. (2019*b*), 'Risk managing tail-risk seekers: Var and expected shortfall vs s-shaped utility', *Journal of Banking & Finance* **101**, 122–135.

Armstrong, J., Brigo, D. & Tse, A. S. (2020), 'The importance of dynamic risk constraints for limited liability operators', *arXiv preprint arXiv:2011.03314* .

Basak, S. & Shapiro, A. (2001), 'Value-at-risk-based risk management: optimal policies and asset prices', *The review of financial studies* **14**(2), 371–405.

Baser, O. (2007), 'Modeling transformed health care cost with unknown heteroskedasticity', *Applied Economics Research* **1**, 1–6.

Bellman, R. (1966), 'Dynamic programming', *Science* **153**(3731), 34–37.

Cuoco, D., He, H. & Isaenko, S. (2008), 'Optimal dynamic trading strategies with risk limits', *Operations Research* **56**(2), 358–368.

Denault, M., Delage, E. & Simonato, J.-G. (2017), 'Dynamic portfolio choice: a simulation-and-regression approach', *Optimization and Engineering* **18**(2), 369–406.

Dong, Y. & Zheng, H. (2019), 'Optimal investment of dc pension plan under short-selling constraints and portfolio insurance', *Insurance: Mathematics and Economics* **85**, 47–59.

Duan, N. (1983), 'Smearing estimate: a nonparametric retransformation method', *Journal of the American Statistical Association* **78**(383), 605–610.

Harvey, A. C. (1976), 'Estimating regression models with multiplicative heteroscedasticity', *Econometrica: Journal of the Econometric Society* pp. 461–465.

Hu, Y. (2013), 'American spread option models and valuation', *Brigham Young University-Provo* .

Kahneman, D. & Tversky, A. (2013), Prospect theory: An analysis of decision under risk, *in* 'Handbook of the fundamentals of financial decision making: Part I', World Scientific, pp. 99–127.

Karatzas, I., Lehoczky, J. P. & Shreve, S. E. (1987), 'Optimal portfolio and consumption decisions for a "small investor" on a finite horizon', *SIAM journal on control and optimization* **25**(6), 1557–1586.

Kharroubi, I., Langrené, N. & Pham, H. (2014), 'A numerical algorithm for fully nonlinear hjb equations: an approach by control randomization', *Monte Carlo Methods and Applications* **20**(2), 145–165.

Longstaff, F. A. & Schwartz, E. S. (2001), 'Valuing american options by simulation: a simple least-squares approach', *The review of financial studies* **14**(1), 113–147.

Samuelson, P. A. (1975), 'Lifetime portfolio selection by dynamic stochastic programming', *Stochastic Optimization Models in Finance* pp. 517–524.

Yiu, K.-F. C. (2004), 'Optimal portfolios under a value-at-risk constraint', *Journal of Economic Dynamics and Control* **28**(7), 1317–1334.

Zhang, R., Langrené, N., Tian, Y., Zhu, Z., Klebaner, F. & Hamza, K. (2019), 'Skewed target range strategy for multiperiod portfolio optimization using a two-stage least squares monte carlo method', *Journal of Computational Finance, Forthcoming* .

Zhou, X.-H., Lin, H. & Johnson, E. (2008), 'Non-parametric heteroscedastic transformation regression models for skewed data with an application to health care costs', *Journal of the Royal Statistical Society: Series B (Statistical Methodology)* **70**(5), 1029–1047.

Ye_Baofeng_01918592

GRADEMARK REPORT

FINAL GRADE

/0

GENERAL COMMENTS

Instructor

PAGE 1

PAGE 2

PAGE 3

PAGE 4

PAGE 5

PAGE 6

PAGE 7

PAGE 8

PAGE 9

PAGE 10

PAGE 11

PAGE 12

PAGE 13

PAGE 14

PAGE 15

PAGE 16

PAGE 17

PAGE 18

PAGE 19

PAGE 20

PAGE 21

PAGE 22

PAGE 23

PAGE 24

PAGE 25

PAGE 26

PAGE 27

PAGE 28

PAGE 29

PAGE 30

PAGE 31

PAGE 32

PAGE 33

PAGE 34

PAGE 35

PAGE 36

PAGE 37

PAGE 38

PAGE 39

PAGE 40

PAGE 41

PAGE 42

PAGE 43

PAGE 44

PAGE 45

PAGE 46